

Inleiding Subatomaire Fysica

Frank Filthaut

<http://www.hef.ru.nl/~filthaut/teach/isaf/welcome.php>:

course information, including lecture notes

Course Contents

1. Introduction

2. Quantum Electrodynamics

- heuristic derivation of Feynman diagrams

3. Strong Interaction and Quantum Chromodynamics

- hadrons and the static quark model
- dynamics: deep-inelastic scattering
- QCD

4. Weak Interaction

- leptons: unitarity, gauge bosons
- Higgs mechanism
- quarks: CKM-matrix, discrete symmetries, CP violation
- (neutrino oscillations)

Course Strategy

Main aim: explain how the Standard Model “works”

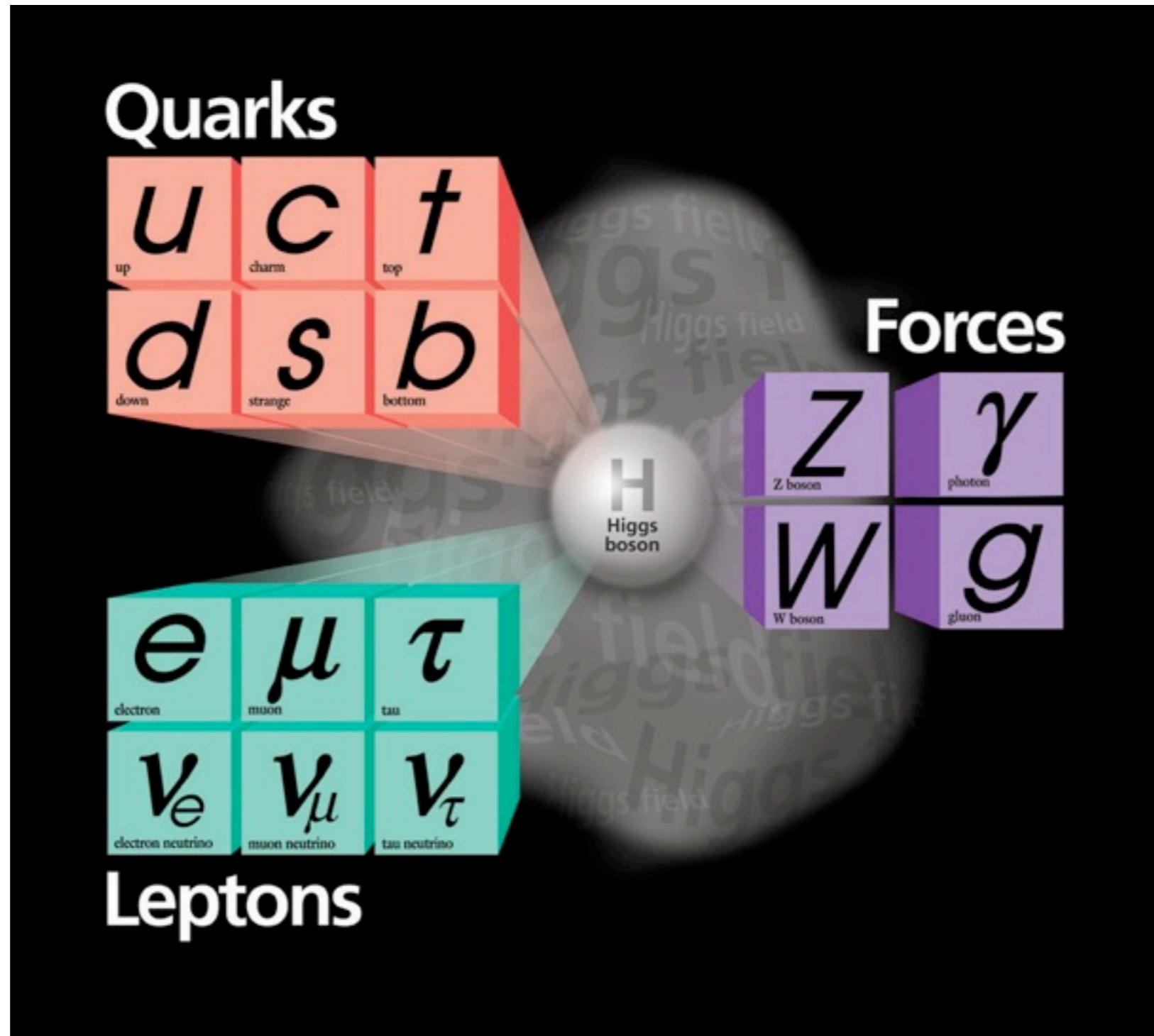
Emphasis on theoretical aspects

- but information from experiment is indispensable! Wherever relevant or useful, experimental results will be discussed

No time for aspects of instrumentation

- but see next pages for generally relevant properties

Particles in the Standard Model



Current Research

The Standard Model is extraordinarily successful in describing elementary particles and their EM, weak, and strong interactions...
but it is incomplete!

The Higgs boson has not been found yet

- an important research topic

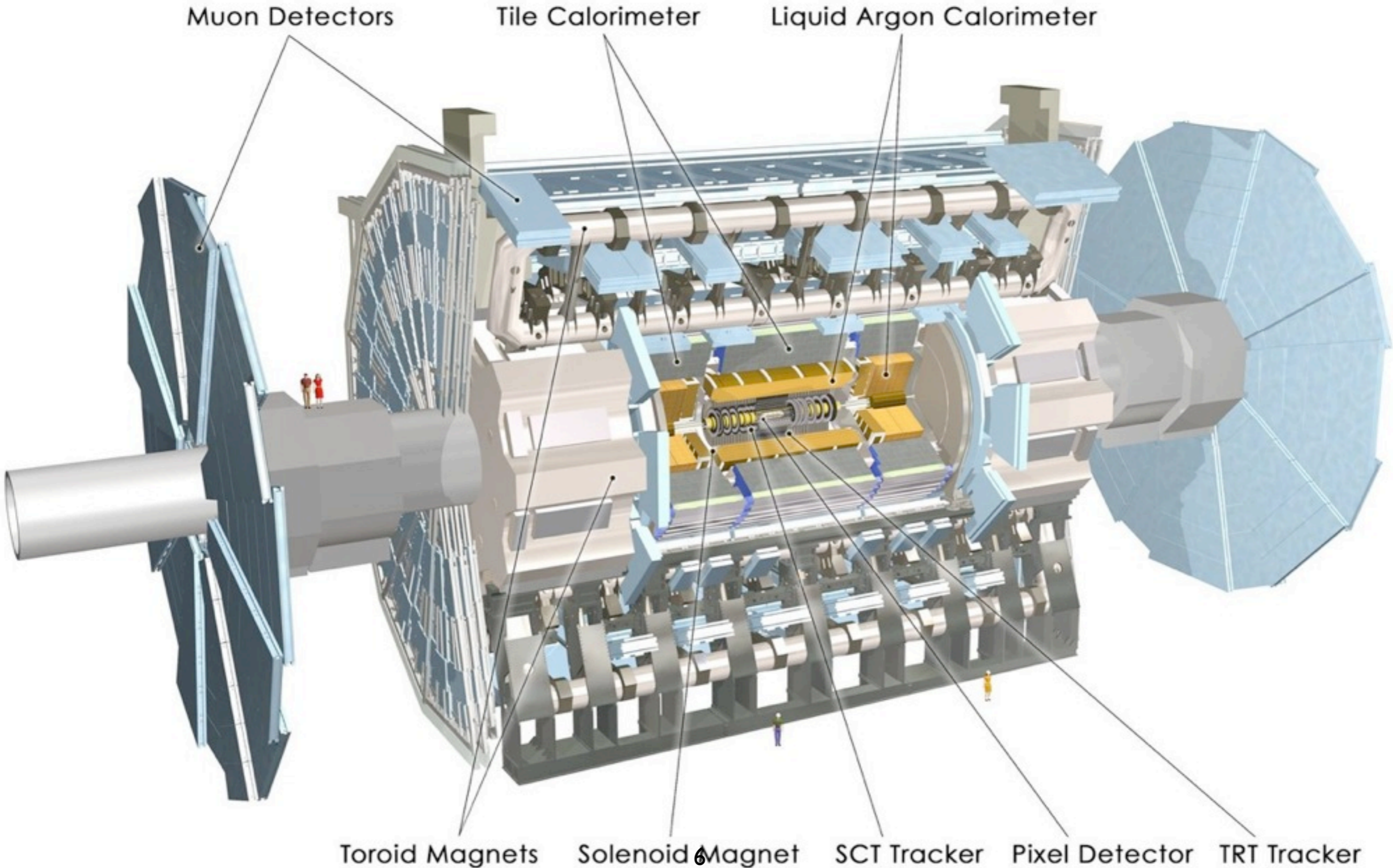
There are theoretical problems (“fine tuning” / “hierarchy”) related to the Higgs boson, and the Standard Model cannot describe gravitation

- searches for experimental evidence for models for “beyond the Standard Model” physics

The Standard Model does not explain the existence of dark matter and dark energy

- interaction with astrophysics (cosmology, ...)

Not an Aim: understanding of detectors



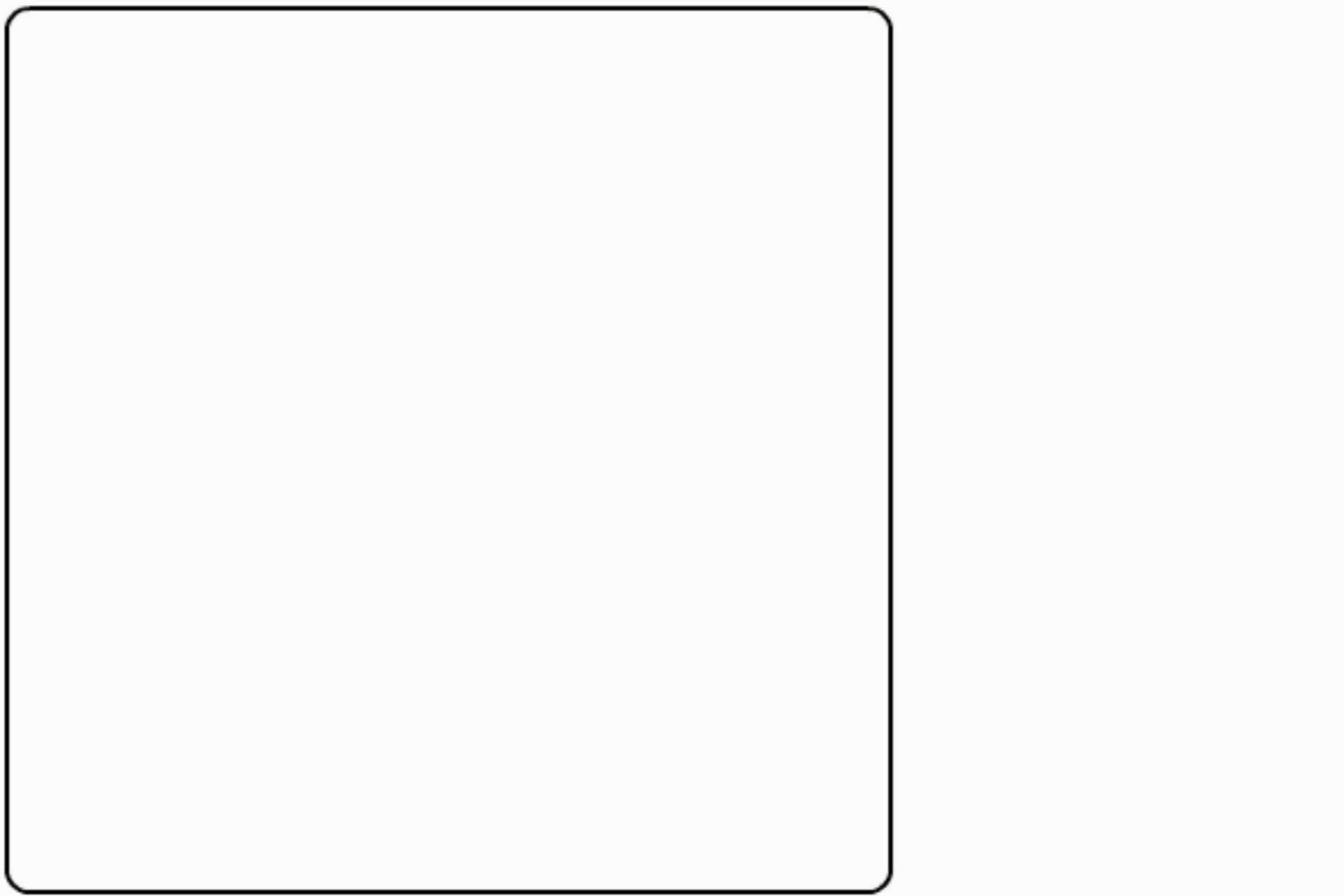
But: which particles are measured?

Typical functionality of a multi-purpose collider detector (see animation):

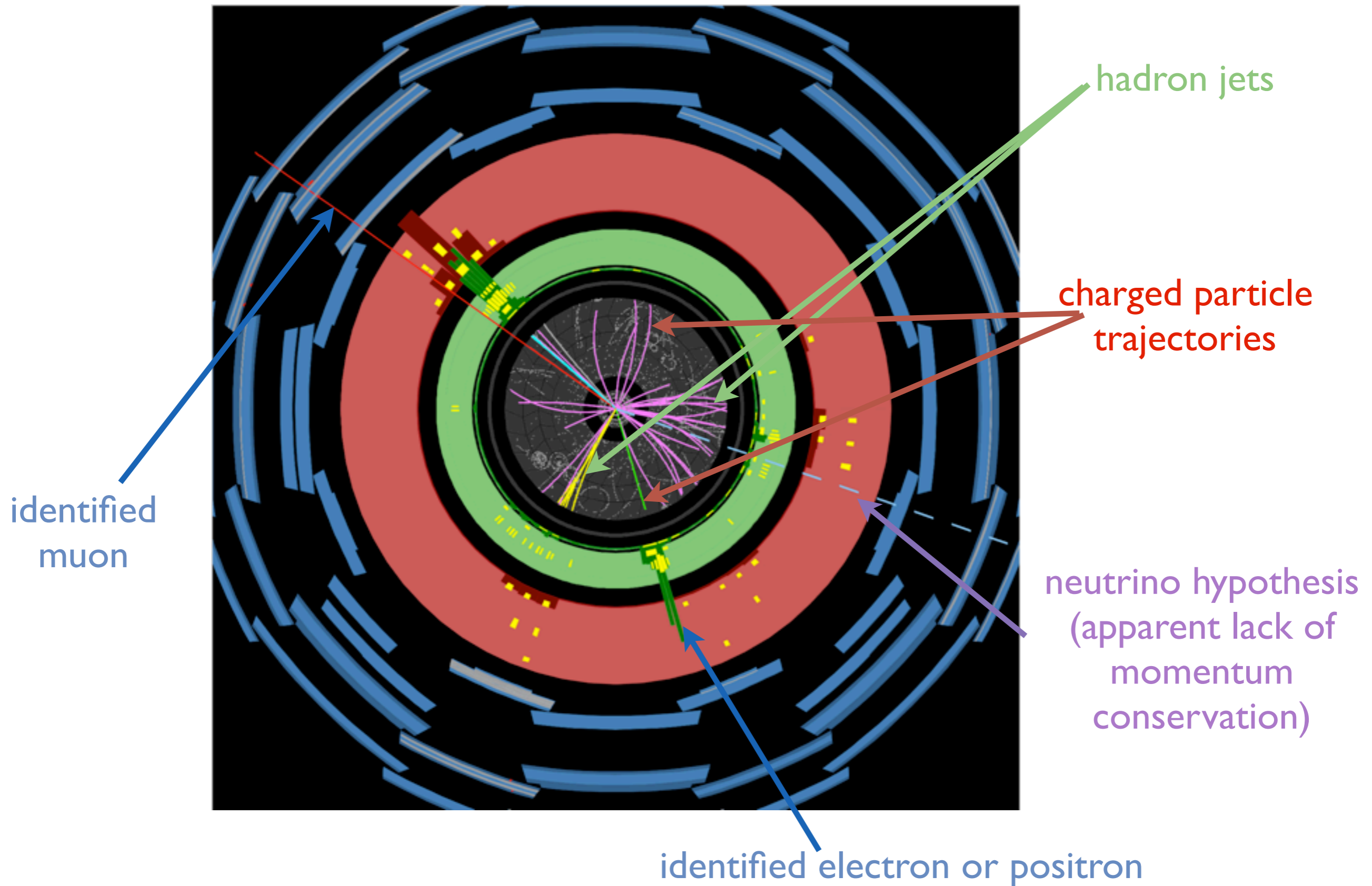
- charged particles are identified and their momenta measured in **tracking detectors**
- electrons, positrons, and photons are absorbed, identified, and their energy measured in the **electromagnetic calorimeter**
- strongly interacting particles (hadrons) are absorbed and their energy measured in the **hadronic calorimeter**
- muons are identified (and, in some experiments, their momentum measured) in the **muon system**
- short-lived particles are **reconstructed through their decay products**
- (high-energy) quarks/gluons manifest themselves as **hadron jets**
- **neutrinos escape undetected**

We will also encounter examples of detectors with more specific measurement purposes

Atlas Experiment: Animation



Example: Event Display



Non-relativistic: Schrödinger equation

$$i \frac{\partial}{\partial t} \psi(\vec{x}) = \left(-\frac{\vec{\nabla}^2}{2m} + V(x) \right) \psi(\vec{x})$$

multiply by ψ^*

$$-i \frac{\partial}{\partial t} \psi^*(\vec{x}) = \left(-\frac{\vec{\nabla}^2}{2m} + V(x) \right) \psi^*(\vec{x})$$

multiply by ψ

$$i \left(\psi^*(\vec{x}) \frac{\partial}{\partial t} \psi(\vec{x}) + \psi(\vec{x}) \frac{\partial}{\partial t} \psi^*(\vec{x}) \right) = -\frac{1}{2m} \left(\psi^*(\vec{x}) \vec{\nabla}^2 \psi(\vec{x}) - \psi(\vec{x}) \vec{\nabla}^2 \psi^*(\vec{x}) \right)$$

$$i \frac{\partial}{\partial t} |\psi(\vec{x})|^2 = -\frac{1}{2m} \vec{\nabla} \cdot \left(\psi^*(\vec{x}) \vec{\nabla} \psi(\vec{x}) - \psi(\vec{x}) \vec{\nabla} \psi^*(\vec{x}) \right).$$

Continuity equation:

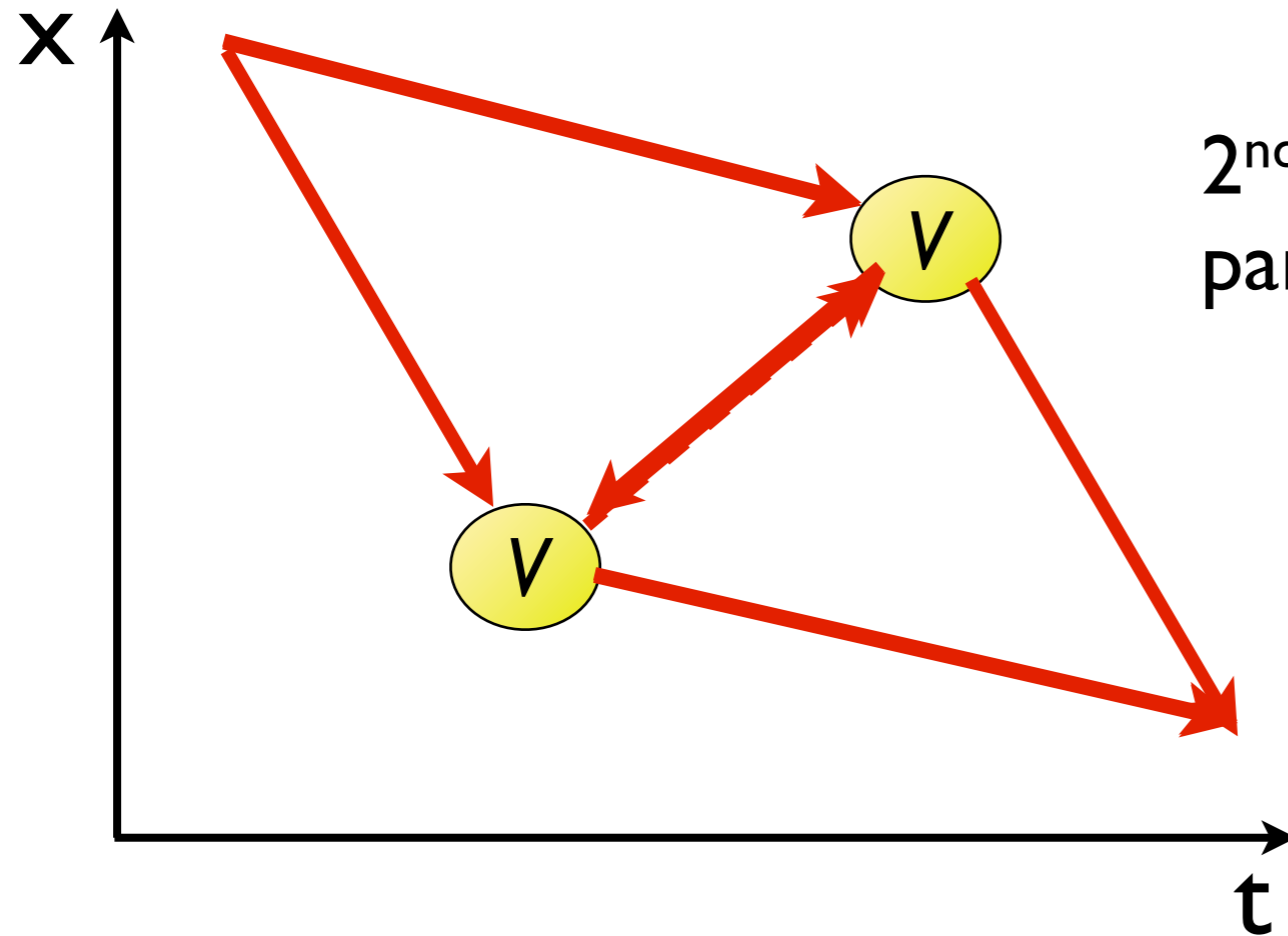
$$\frac{\partial}{\partial t} \rho(\vec{x}) + \vec{\nabla} \cdot \vec{j}(\vec{x}) = 0$$

$$\rho(\vec{x}) = |\psi(\vec{x})|^2,$$

$$\vec{j}(\vec{x}) = \frac{-i}{2m} \left(\psi^*(\vec{x}) \vec{\nabla} \psi(\vec{x}) - \psi(\vec{x}) \vec{\nabla} \psi^*(\vec{x}) \right)$$

Week 2

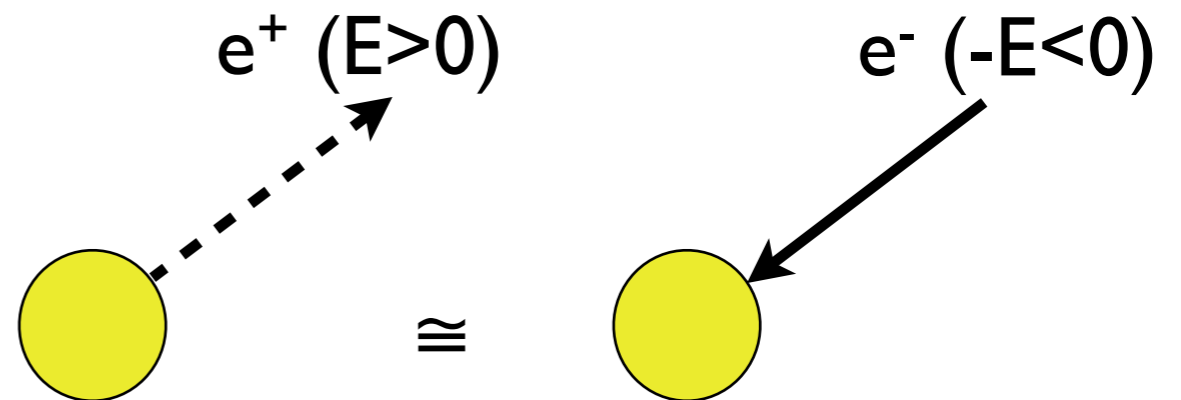
Negative-energy solutions



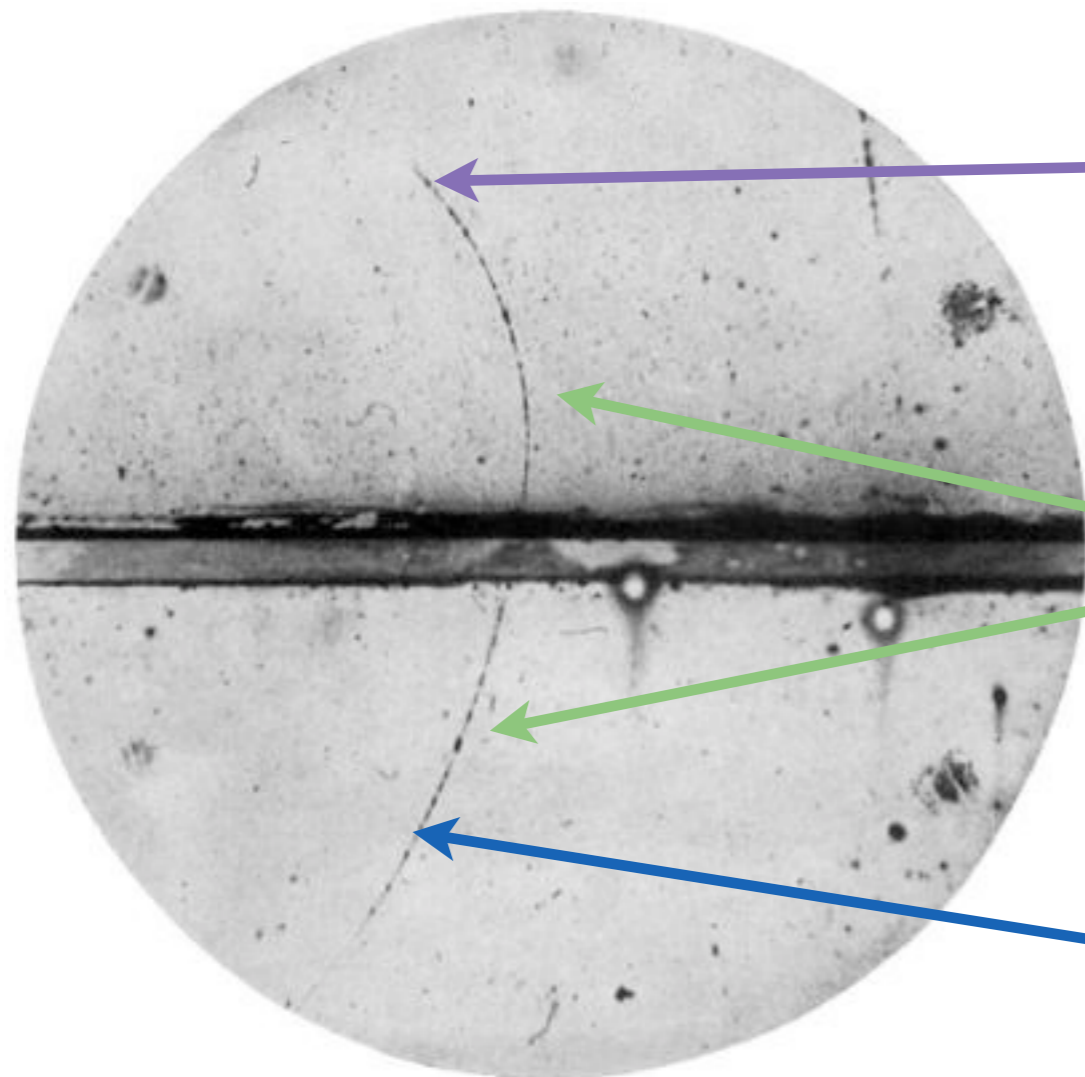
2nd order process: scattering of a particle off of two potentials

Identical effect on “the system” (quantum numbers):

- emission of an anti-particle
- absorption of a ($E < 0$) particle



Discovery of the positron



Path length much longer than expected for protons: a light particle

Larger curvature above than below the Pb plate: particle travels upward

Sign of the curvature in the B-field: positively charged particle

FIG. 1. A 63 million volt positron ($H\rho = 2.1 \times 10^6$ gauss-cm) passing through a 6 mm lead plate and emerging as a 23 million volt positron ($H\rho = 7.5 \times 10^6$ gauss-cm). The length of this latter path is at least ten times greater than the possible length of a proton path of this curvature.

Perturbation theory

Add perturbation term V to system H_0 which can be solved completely:

$$H = H_0 + V(\vec{x}, t), \quad H_0\phi_n = E_n\phi_n \quad \text{with} \quad \int d^3x \phi_n^*(\vec{x})\phi_m(\vec{x}) = \delta_{nm}.$$

Expand wavefunction in terms of unperturbed basis:

$$\psi(\vec{x}, t) = \sum_n a_n(t)\phi_n(\vec{x})e^{-iE_nt}.$$

This yields an equation describing the time evolution of the respective coefficients:

$$\begin{aligned} i\frac{\partial\psi(\vec{x}, t)}{\partial t} &= \sum_n \phi_n(\vec{x})e^{-iE_nt} \left(E_n a_n(t) + \frac{da_n(t)}{dt} \right) \\ &= (H_0 + V(\vec{x}, t))\psi = \sum_n (H_0 + V(\vec{x}, t))a_n(t)\phi_n(\vec{x})e^{-iE_nt} \\ &= \sum_n (E_n + V(\vec{x}, t))a_n(t)\phi_n(\vec{x})e^{-iE_nt} \\ \Rightarrow i \sum_n \frac{da_n(t)}{dt} \phi_n(\vec{x})e^{-iE_nt} &= \sum_n V(\vec{x}, t)a_n(t)\phi_n(\vec{x})e^{-iE_nt} \end{aligned}$$

Perturbation theory (2)

Multiply by $\phi_f^* e^{iE_f t}$ and integrate over space:

$$\frac{da_f(t)}{dt} = -i \sum_n a_n(t) e^{-i(E_n - E_f)t} \cdot V_{fn}(t), \quad \text{with} \quad V_{fn}(t) = \int d^3x \phi_f^*(\vec{x}) V(\vec{x}, t) \phi_n(\vec{x})$$

Integrate (formally) over time, assuming initial state i :

$$\begin{aligned} a_f(t) &= \delta_{fi} \\ &+ (-i) \int_{-T}^t dt' V_{fi}(t') e^{-i(E_i - E_f)t'} \\ &+ (-i)^2 \sum_n \int_{-T}^t dt' V_{fn}(t') e^{-i(E_n - E_f)t'} \cdot \int_{-T}^{t'} dt'' V_{ni}(t'') e^{-i(E_i - E_n)t''} + \dots \end{aligned}$$

Make Lorentz-covariant:

$$\phi_n(x) \equiv \phi_n(\vec{x}) e^{-iE_n t} \Rightarrow a_f(t) = -i \int_{-T}^t dt' \int d^3x \phi_f^*(x) V(x) \phi_i(x).$$

This yields:

$$t \rightarrow \infty : T_{fi} \rightarrow -i \int d^4x \phi_f^*(x) V(x) \phi_i(x)$$

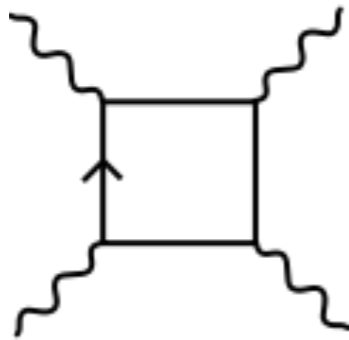
- NB: in the last two equations only **first-order terms** were retained

Week 3

Delbrück scattering

Observed (1973, G. Jarlskog et al.) in scattering of high-energy ($E \sim 7$ GeV) photons off uranium

✱ effect $\sim Z^4$



Small scattering angles (\sim mrad)!

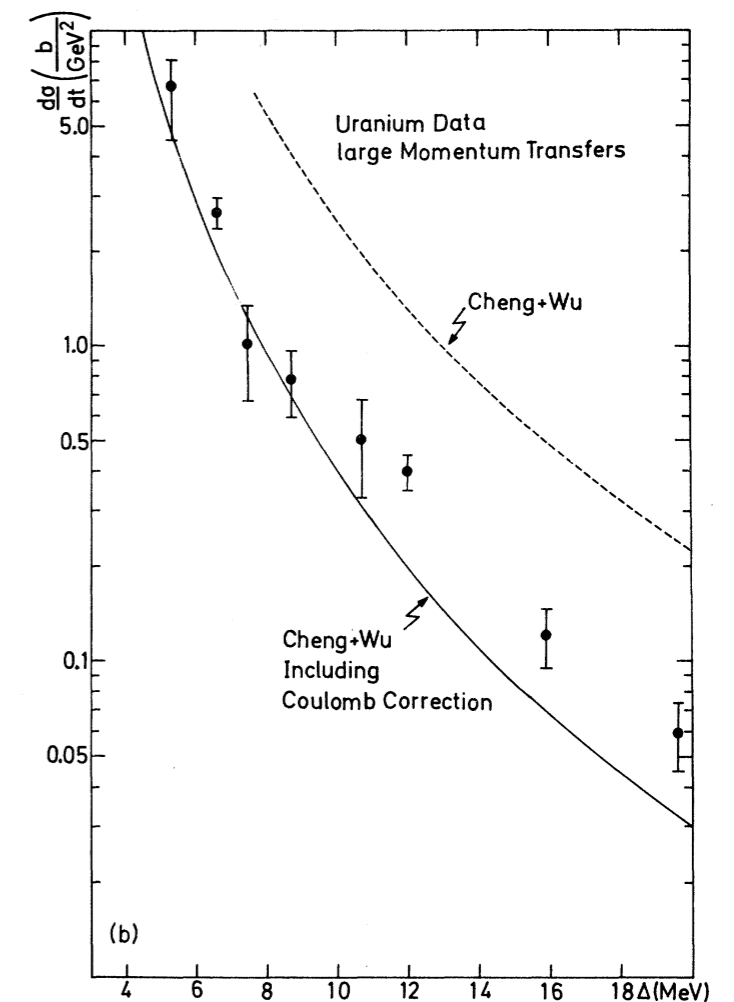
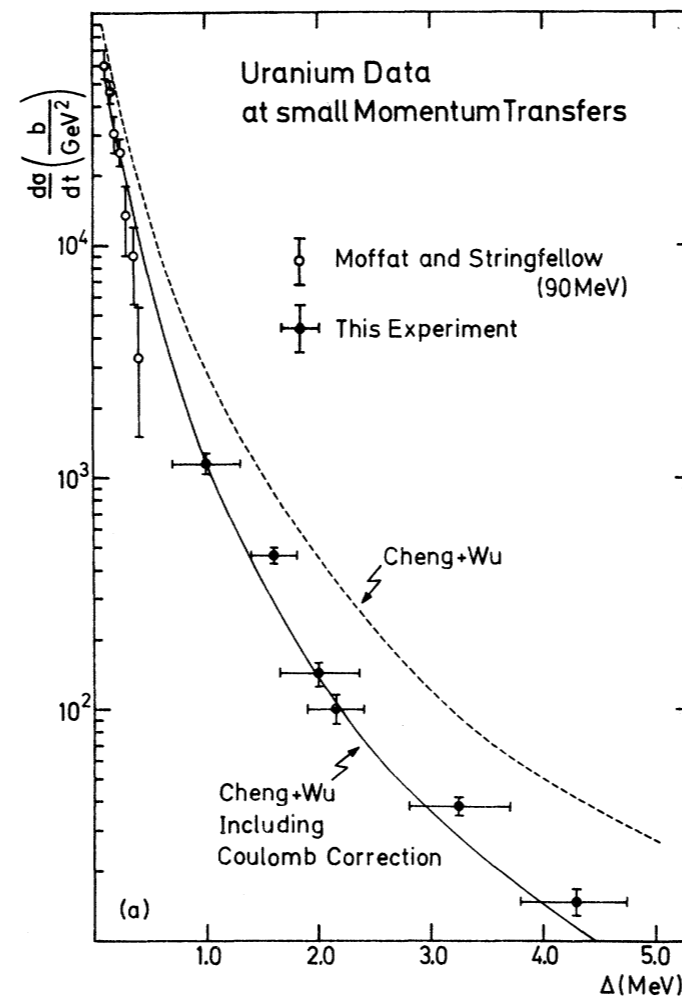


FIG. 9. Measured differential cross sections for Delbrück scattering versus momentum transfer for uranium targets compared to theoretical predictions (Refs. 5 and 16). (a) Small momentum transfers; (b) large momentum transfers.

Electron Magnetic Moment

Dirac equation reduced to two-component spinors:

Spatial (LHS) part:
$$\left(\vec{\sigma} \cdot (\vec{p} + e\vec{A})\right)^2 u_A = ((E + eA^0)^2 - m^2)u_A$$

$$\begin{aligned} \left(\vec{\sigma} \cdot (\vec{p} + e\vec{A})\right)^2 &= \sigma^i \sigma^j \left(p^i p^j + e^2 A^i A^j + e(p^i A^j + A^i p^j)\right) \\ &= (\delta_{ij} + i\epsilon^{ijk} \sigma^k) \left(p^i p^j + e^2 A^i A^j + e(p^i A^j + A^i p^j)\right) \\ &= p^i p^i + e^2 A^i A^i + e(p^i A^i + A^i p^i) + ie(p^i A^j + A^i p^j) \epsilon^{ijk} \sigma^k \\ &= (\vec{p} + e\vec{A})^2 + e(\vec{\nabla} \times \vec{A}) \cdot \vec{\sigma} \\ &= (\vec{p} + e\vec{A})^2 + e\vec{\sigma} \cdot \vec{B} \end{aligned}$$

RHS, non-relativistic limit:

$$((E + eA^0)^2 - m^2) = ((m + (E + eA^0 - m))^2 - m^2) \approx 2m(E + eA^0 - m)$$

Conclusion:

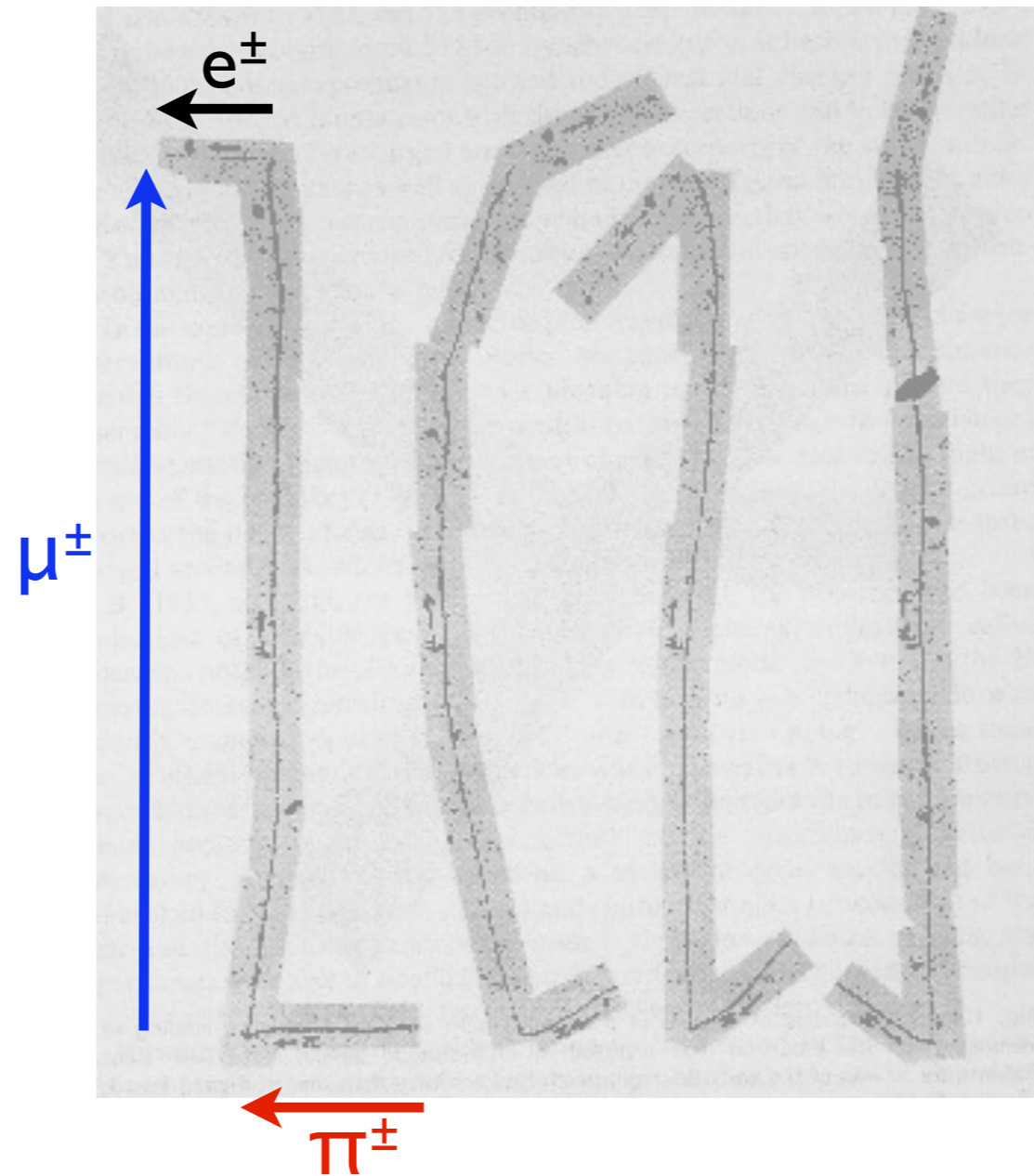
$$(E - m)u_A = \left(\frac{(\vec{p} + e\vec{A})^2}{2m} - eA^0 + \frac{e}{2m} \vec{\sigma} \cdot \vec{B} \right) u_A$$

Week 4

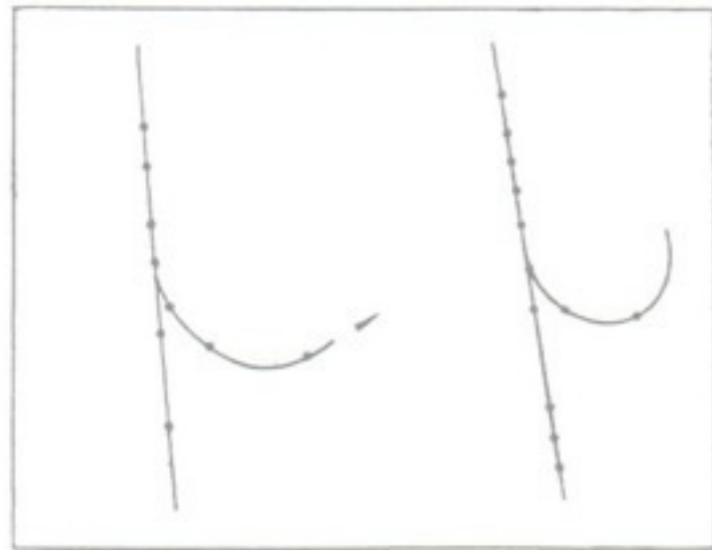
Discovery of the charged pion

(and of the muon...)

1. charged pion is stopped
2. pion decays
3. resulting muon is stopped
4. muon decays
5. electron/positron escapes



Discovery of “strange” particles



Dessin stéréoscopique de la collision.

charged kaon:
angle and energy e^-

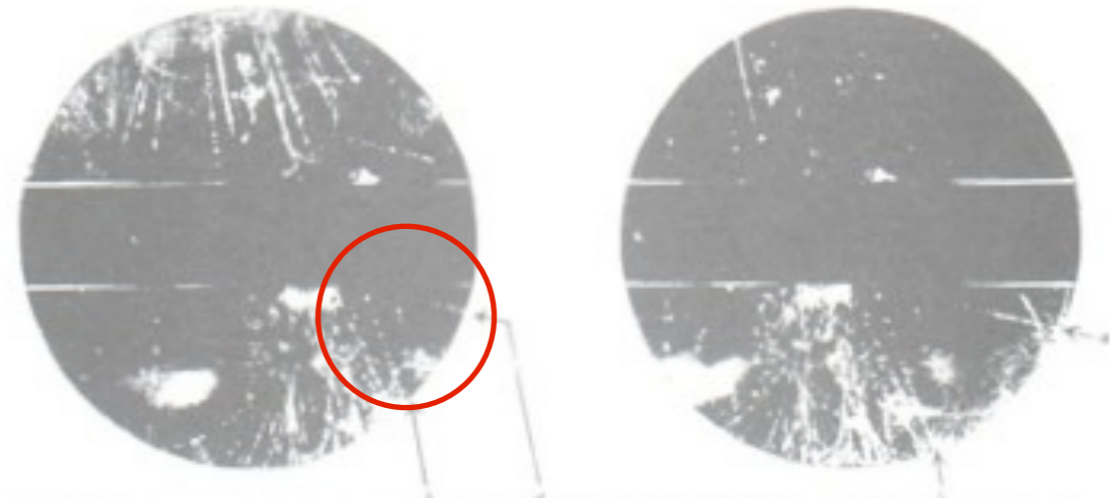


Fig. 1. STEREOSCOPIC PHOTOGRAPHS TAKEN AT CRITICAL POINT IN THE LAB. THE POSITION OF THE MAGNETIC FIELD IS SUCH THAT A POSITIVE PARTICLE CURVES DOWNWARD OR UPWARD IN AN ANTICIPATED MANNER.

V^0 (K_S , Λ): “vertices”,
momenta of outgoing particles

Lifetimes of “strange” particles

particle	mass (MeV)	lifetime (s)	(main) decay modes
spin 0			
K^-	494	$1.2 \cdot 10^{-8}$	$\mu^- \bar{\nu}_\mu, \pi^- \pi^0$
K_S^0	498	$9 \cdot 10^{-11}$	$\pi^+ \pi^-, \pi^0 \pi^0$
K_L^0	498	$5 \cdot 10^{-8}$	$\pi^\pm e^\mp \nu_e, \pi^\pm \mu^\mp \nu_\mu, \pi^+ \pi^- \pi^0, \pi^0 \pi^0 \pi^0$
spin 1/2			
Λ	1116	$2.6 \cdot 10^{-10}$	$p \pi^-, n \pi^0$
Σ^+	1189	$8 \cdot 10^{-11}$	$p \pi^0, n \pi^+$
Σ^0	1193	$7 \cdot 10^{-20}$	$\Lambda \gamma$
Σ^-	1197	$1.5 \cdot 10^{-10}$	$n \pi^-$
Ξ^-	1322	$1.6 \cdot 10^{-10}$	$\Lambda \pi^-$
Ξ^0	1315	$3 \cdot 10^{-10}$	$\Lambda \pi^0$

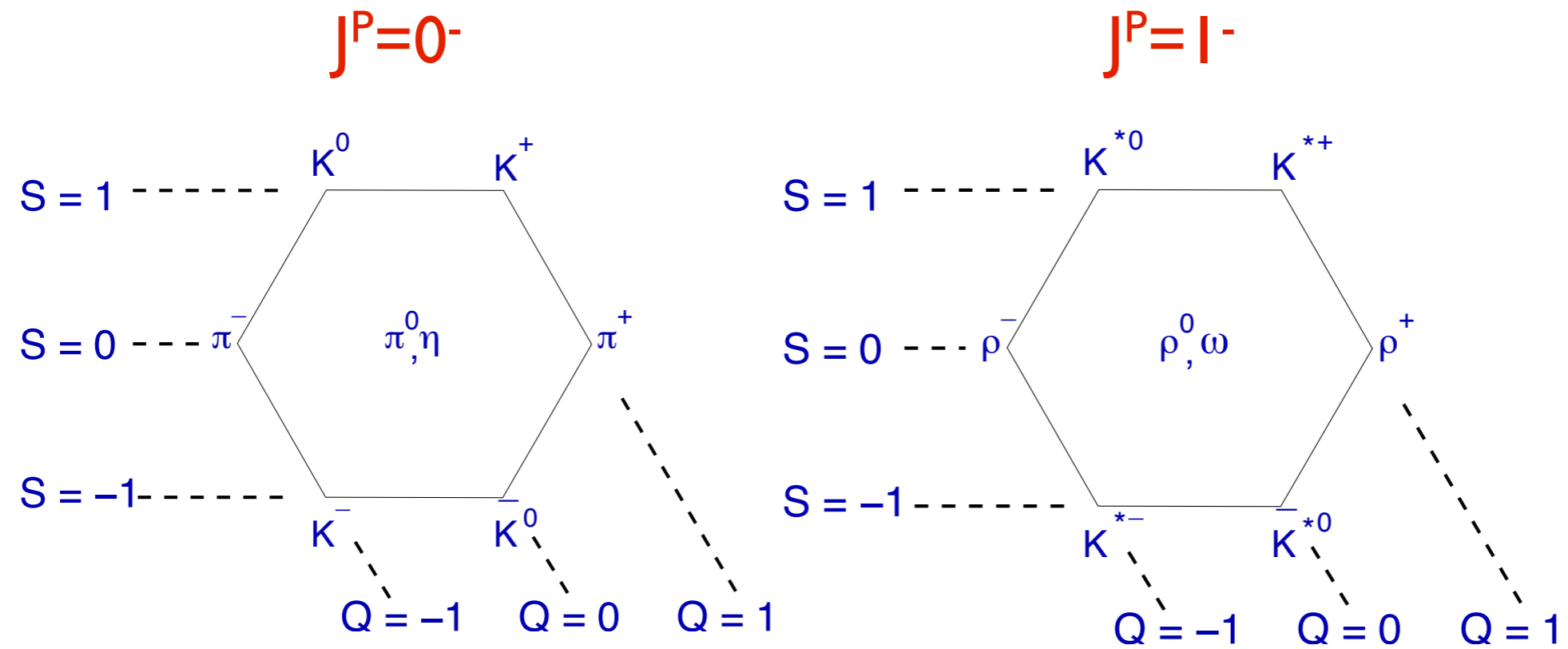
K_S and K_L are “mixtures” of K^0 and \bar{K}^0

• will be covered in context of weak interaction

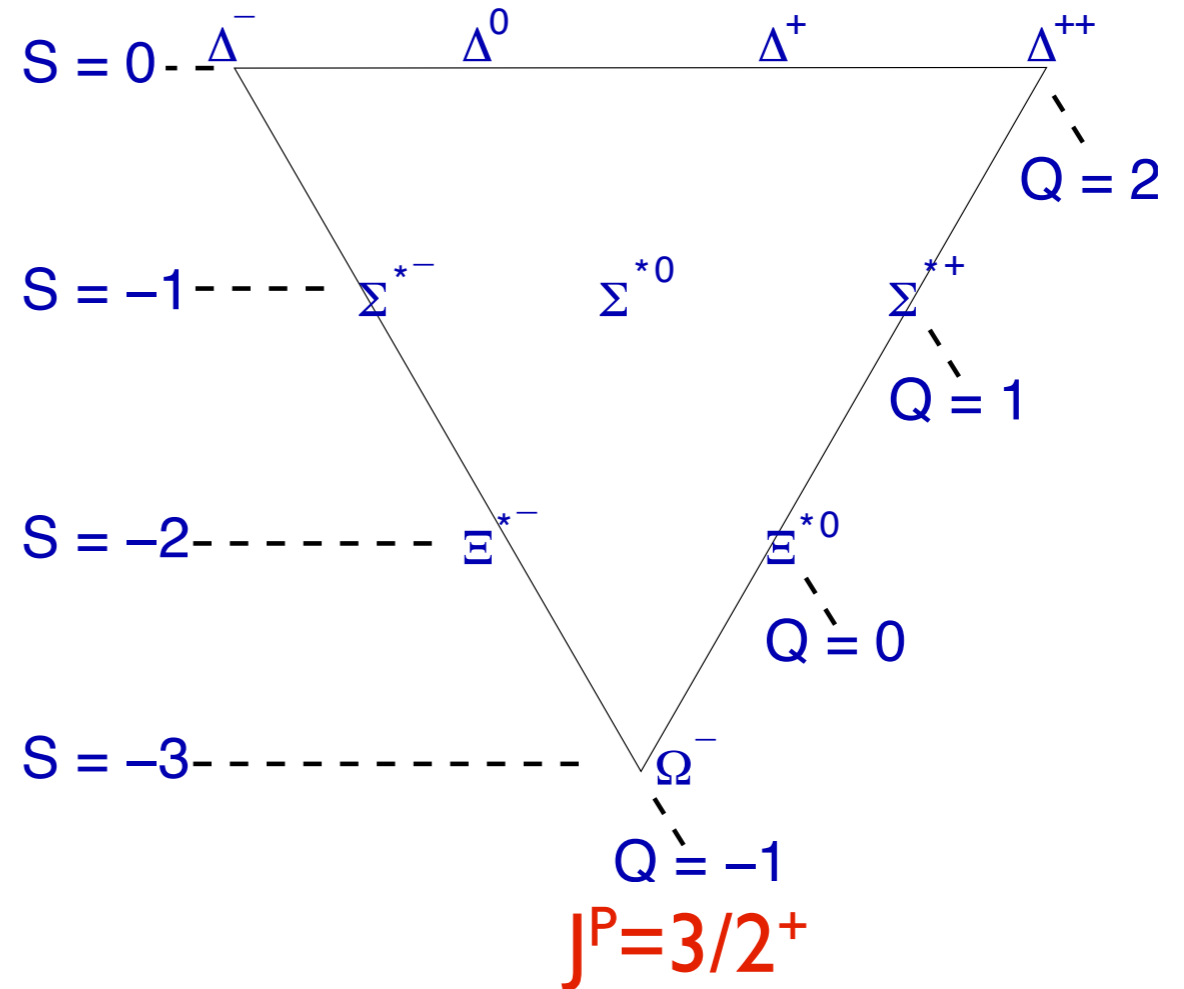
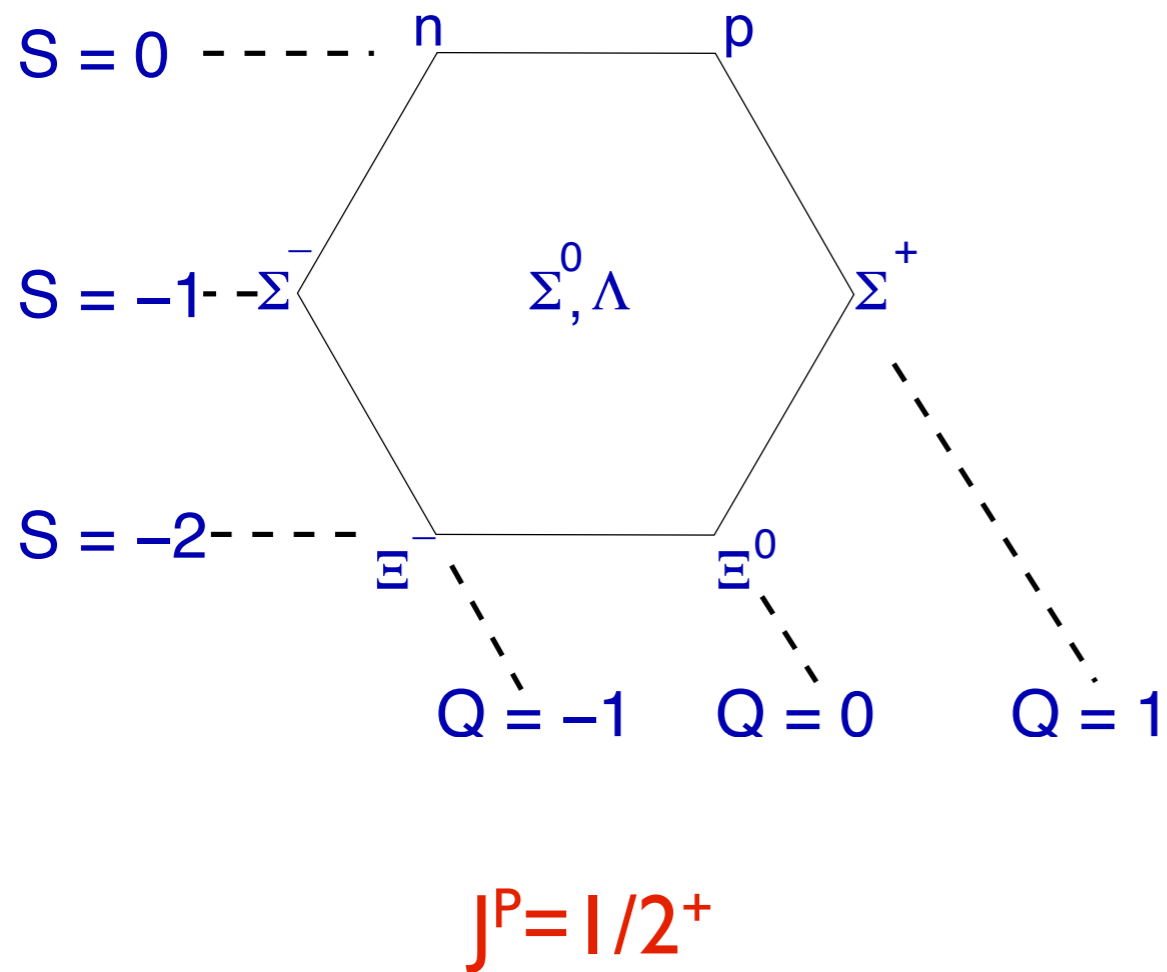
Σ^+, Σ^- are not antiparticles!

Week 5

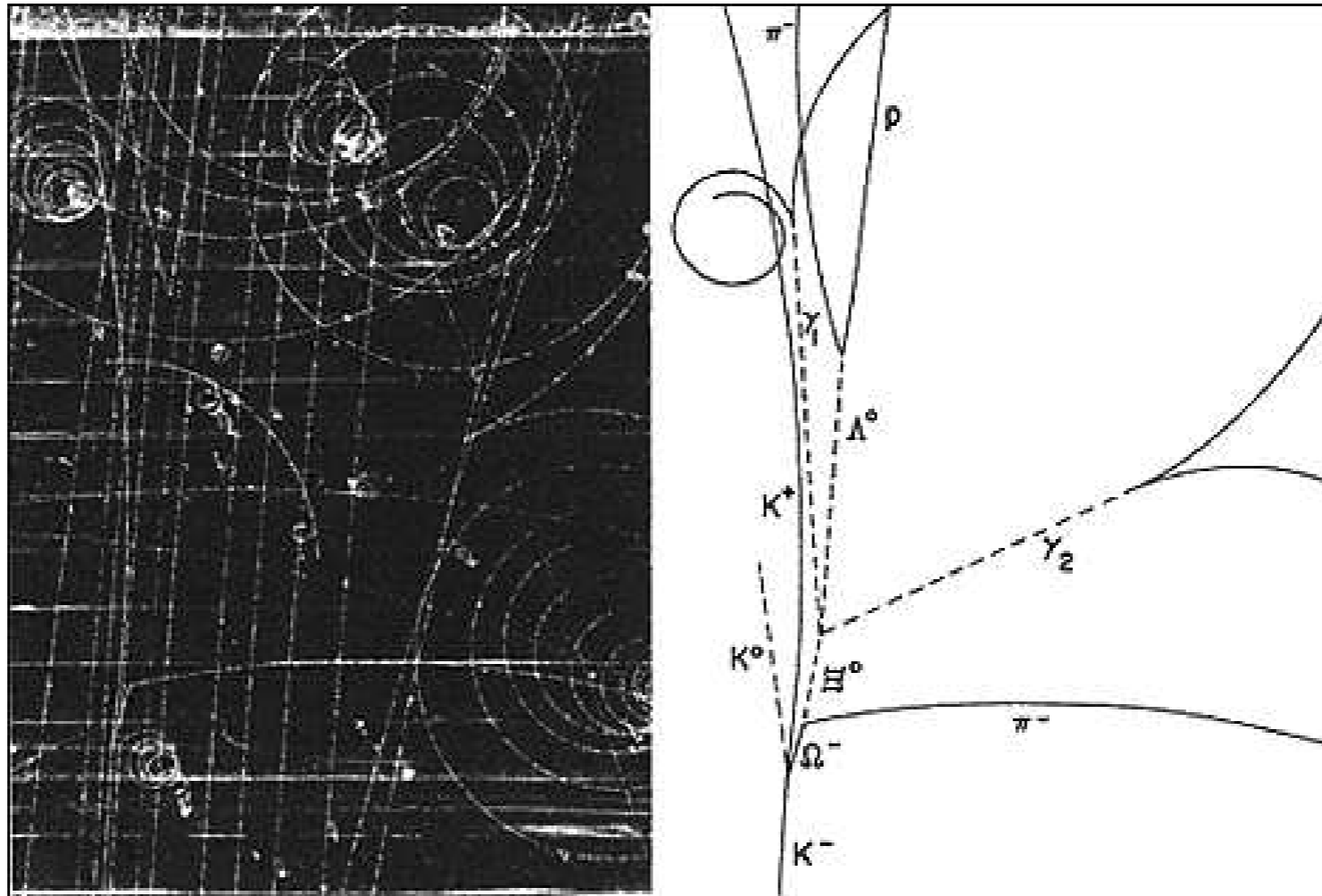
Meson octets



Baryon octet and decuplet



Discovery of the Ω^- particle



Photographed using a “bubble chamber”

- nearly boiling fluid, charged particles cause bubbles

Baryon masses in the spin interaction model

$$M = m_1 + m_2 + m_3 + A \left(\frac{\vec{S}_1 \cdot \vec{S}_2}{m_1 m_2} + \frac{\vec{S}_1 \cdot \vec{S}_3}{m_1 m_3} + \frac{\vec{S}_2 \cdot \vec{S}_3}{m_2 m_3} \right)$$

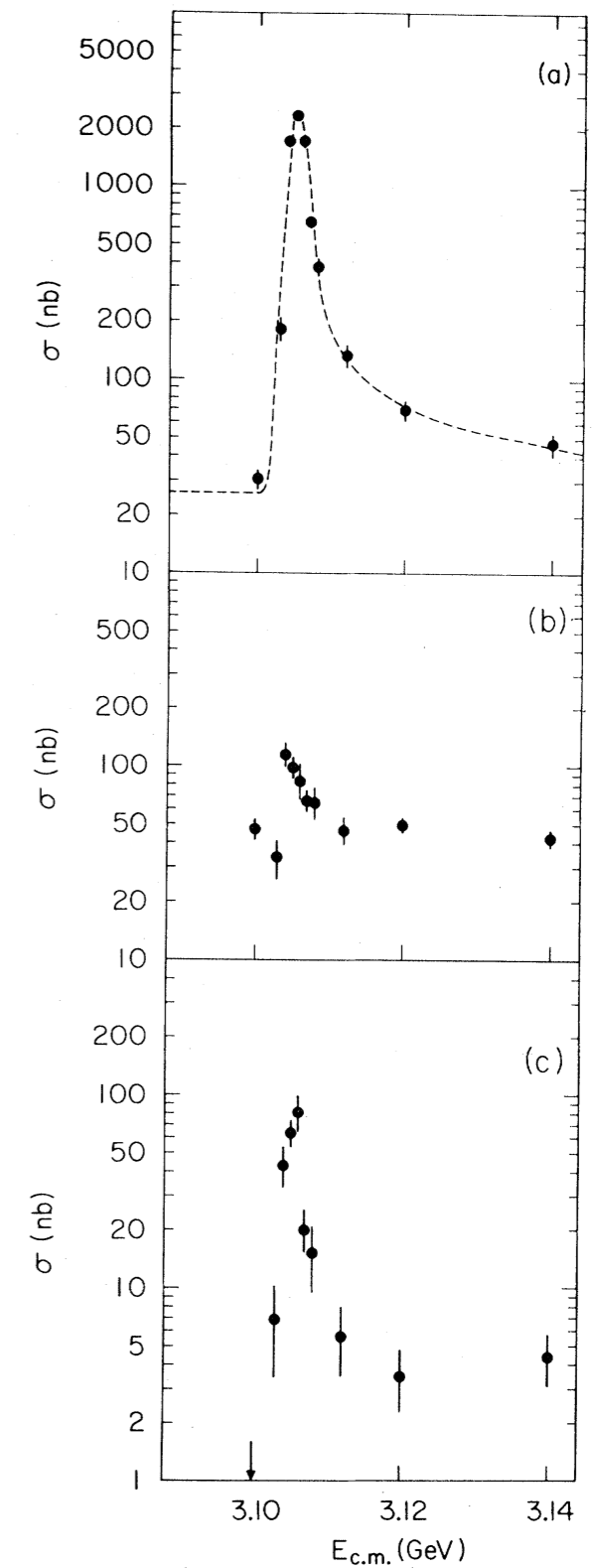
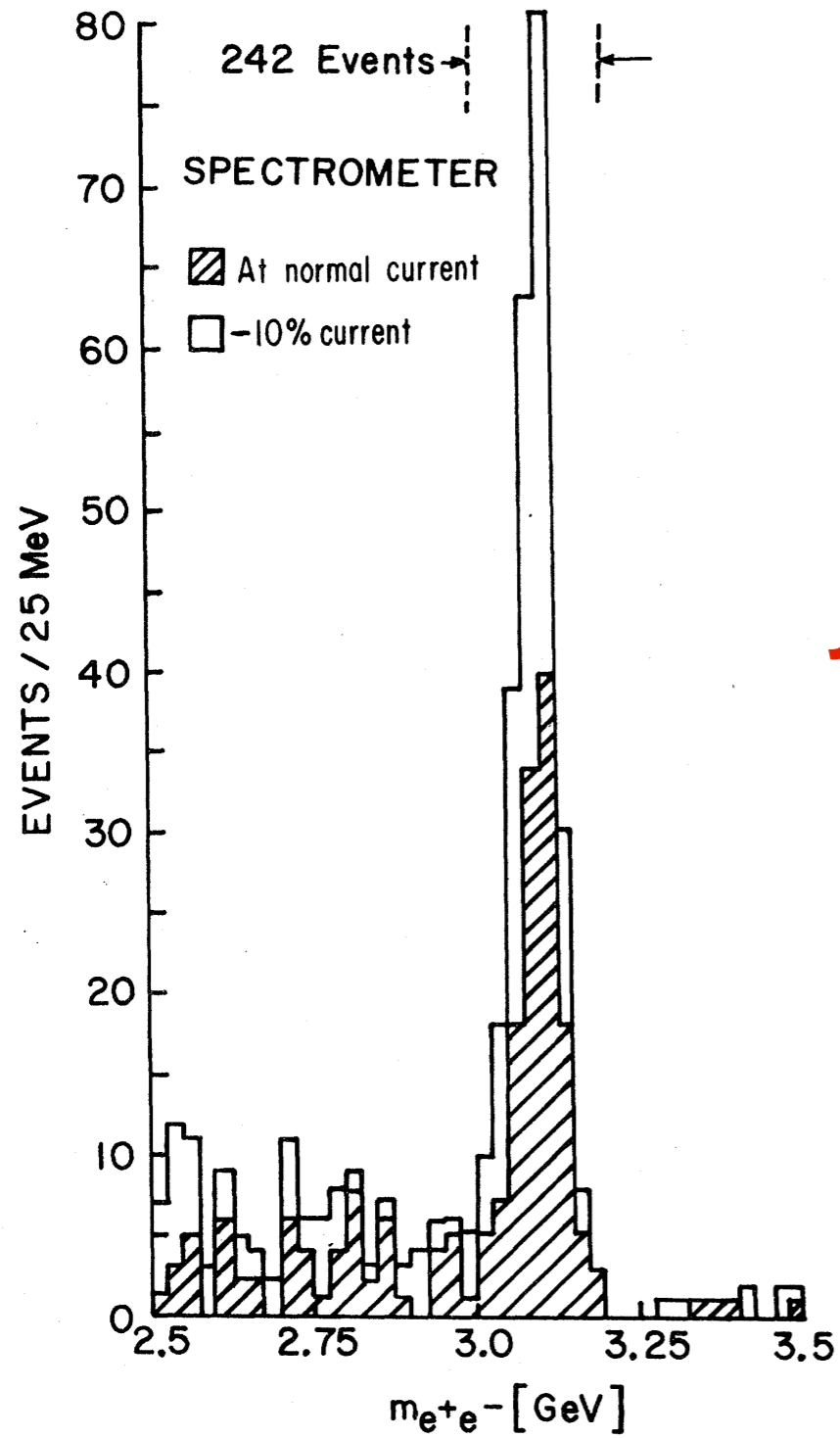
Particle	Predicted mass (GeV)	Measured mass (GeV)
n, p	0.89	0.939
Λ	1.08	1.116
Σ	1.15	1.193
Ξ	1.32	1.318
Δ	1.07	1.232
Σ^*	1.34	1.385
Ξ^*	1.50	1.533
Ω^-	1.68	1.673

Meson masses in the spin interaction model

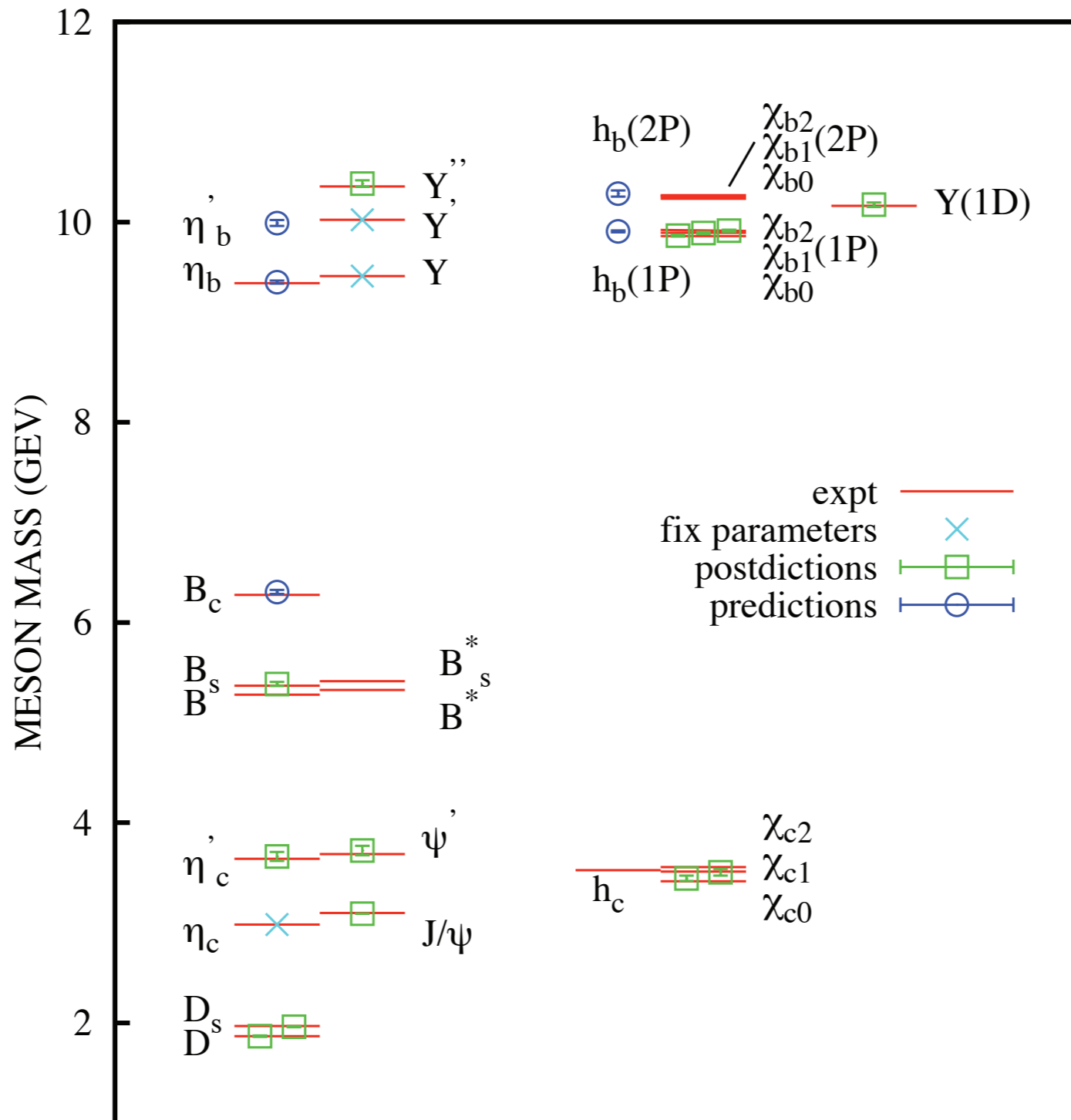
$$M = m_q + m_{\bar{q}} + A' \frac{\vec{S}_q \cdot \vec{S}_{\bar{q}}}{m_q m_{\bar{q}}}$$

Particle	Predicted mass (GeV)	Measured mass (GeV)
π	0.15	0.137
K	0.46	0.496
η	0.57	0.549
ρ	0.77	0.770
ω	0.77	0.782
K^*	0.87	0.892
ϕ	1.03	1.020

Discovery of the J/Ψ particle

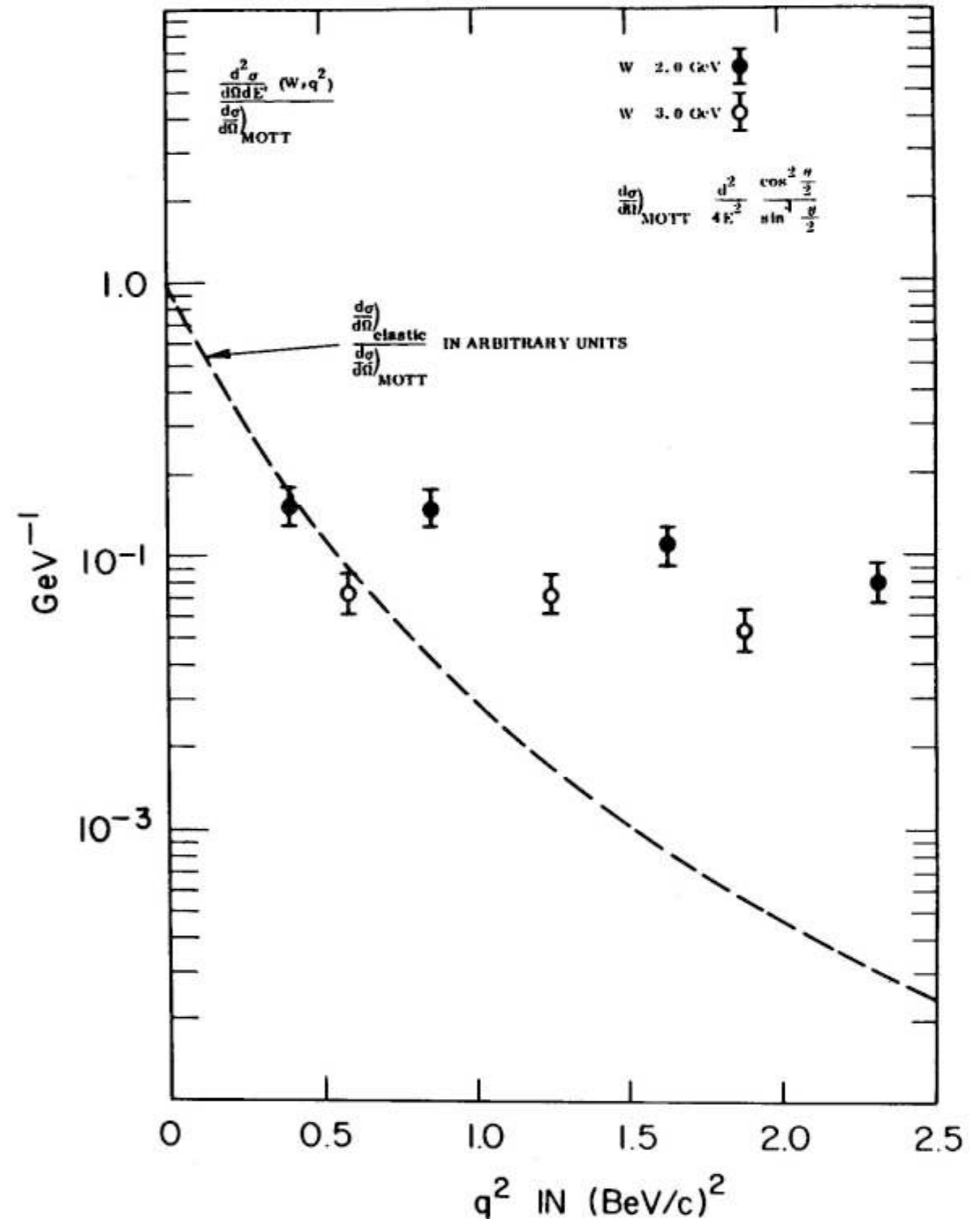


Spectroscopy of heavy mesons



Inelastic electron-proton scattering

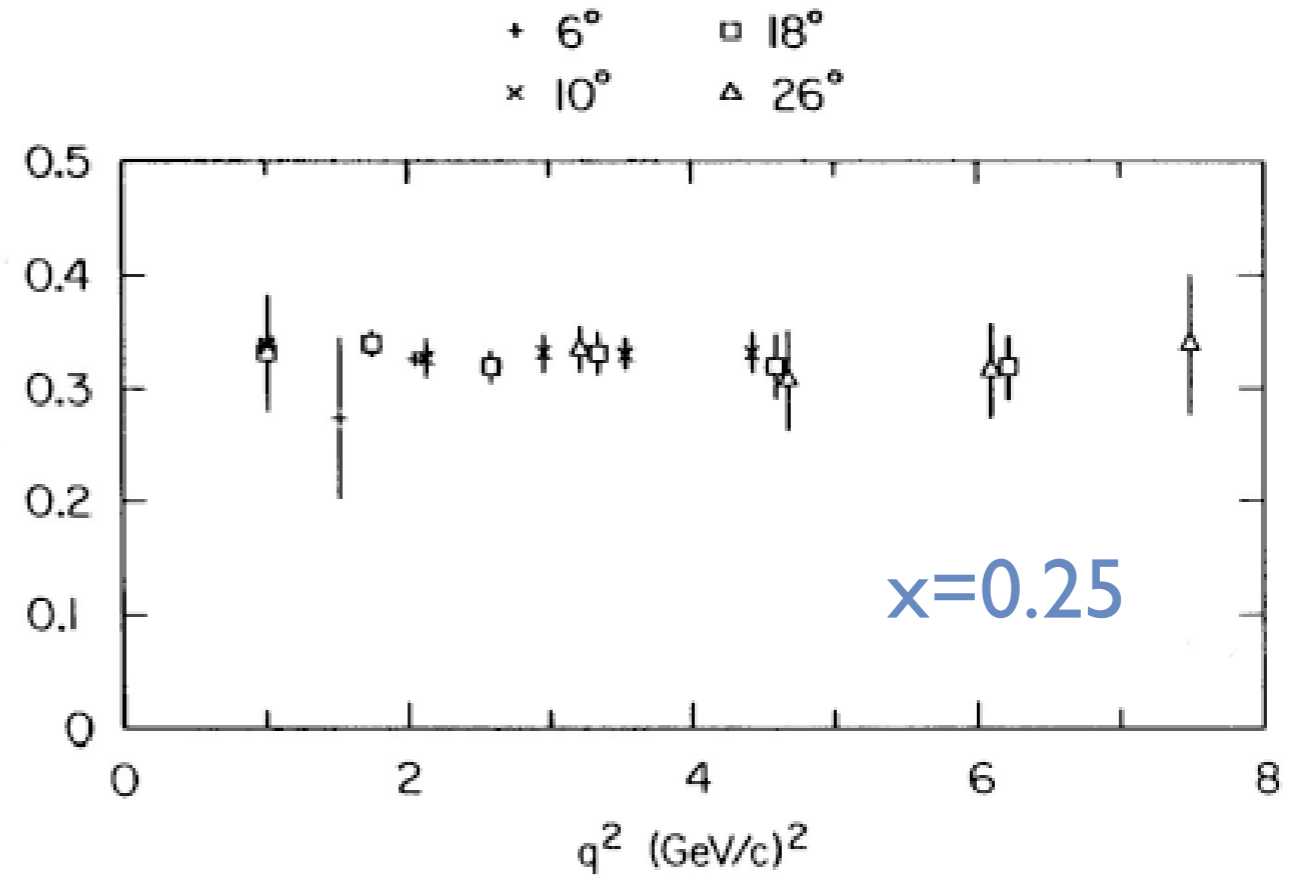
- Experiments by Friedman, Kendall, Taylor et al., 1969:
- $E_e \approx 20 \text{ GeV}$
- measurement of **inclusive cross sections** (i.e., not only e-p final states are being considered)
- **First indication of the proton's composite nature**



Bjorken scaling

Experiment: deep-inelastic
electron-proton scattering,
 $E_e \approx 20 \text{ GeV}$

$$\frac{Q^2}{2m_p x} W_2(x, Q^2)^{1/2}$$



Week 6

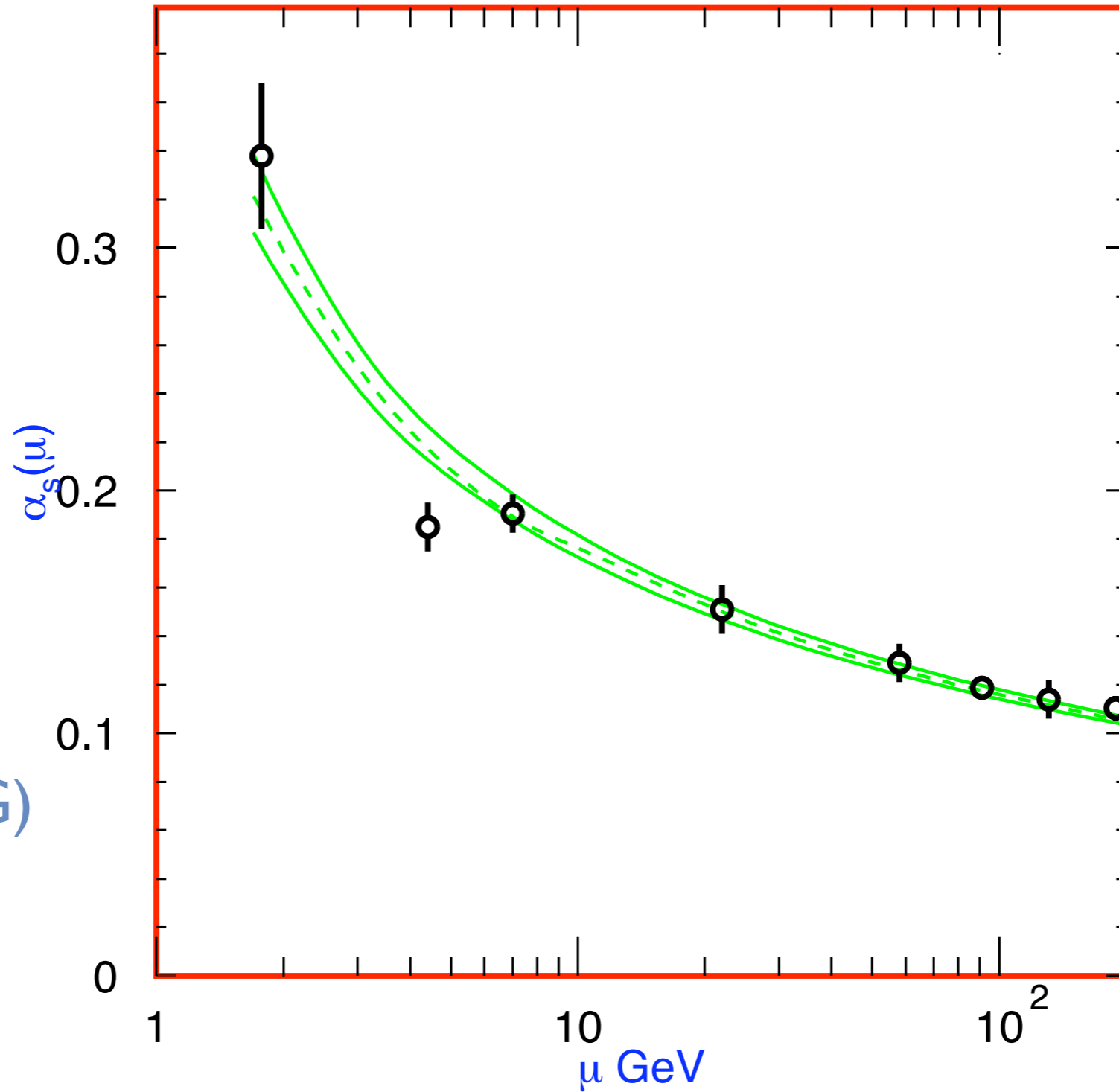
Gell-Mann matrices

$$\lambda^1 = \begin{pmatrix} 0 & 1 & 0 \\ 1 & 0 & 0 \\ 0 & 0 & 0 \end{pmatrix}$$
$$\lambda^4 = \begin{pmatrix} 0 & 0 & 1 \\ 0 & 0 & 0 \\ 1 & 0 & 0 \end{pmatrix}$$
$$\lambda^7 = \begin{pmatrix} 0 & 0 & 0 \\ 0 & 0 & -i \\ 0 & i & 0 \end{pmatrix}$$

$$\lambda^2 = \begin{pmatrix} 0 & -i & 0 \\ i & 0 & 0 \\ 0 & 0 & 0 \end{pmatrix}$$
$$\lambda^5 = \begin{pmatrix} 0 & 0 & -i \\ 0 & 0 & 0 \\ i & 0 & 0 \end{pmatrix}$$
$$\lambda^8 = \frac{1}{\sqrt{3}} \begin{pmatrix} 1 & 0 & 0 \\ 0 & 1 & 0 \\ 0 & 0 & -2 \end{pmatrix}$$

$$\lambda^3 = \begin{pmatrix} 1 & 0 & 0 \\ 0 & -1 & 0 \\ 0 & 0 & 0 \end{pmatrix}$$
$$\lambda^6 = \begin{pmatrix} 0 & 0 & 0 \\ 0 & 0 & 1 \\ 0 & 1 & 0 \end{pmatrix}$$

Q^2 dependence of α_s

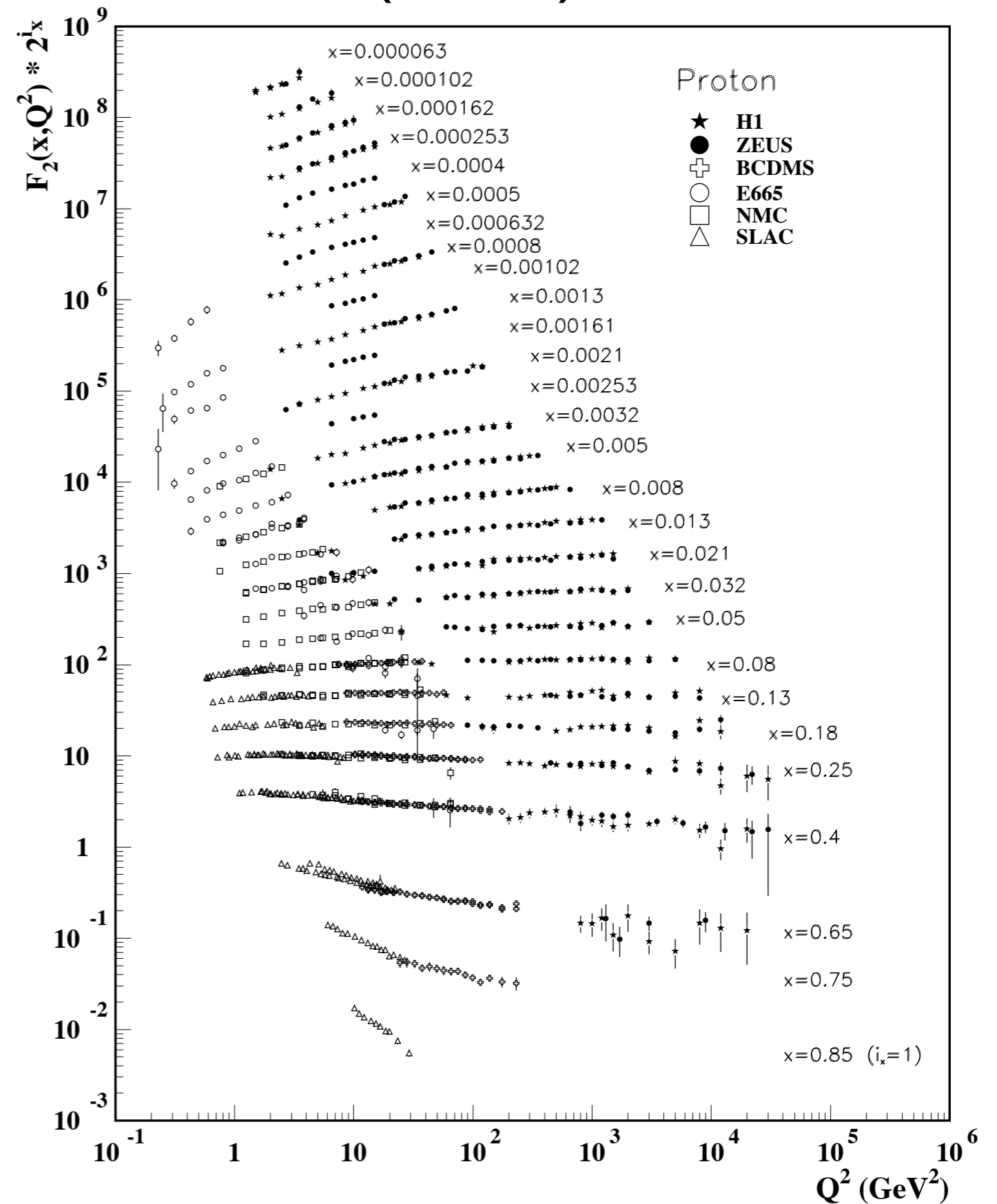


(source: PDG)

Measurements of $F_2(x, Q^2)$

- log-log scale!
- data for different values of x moved by a factor 2^i (for readability)

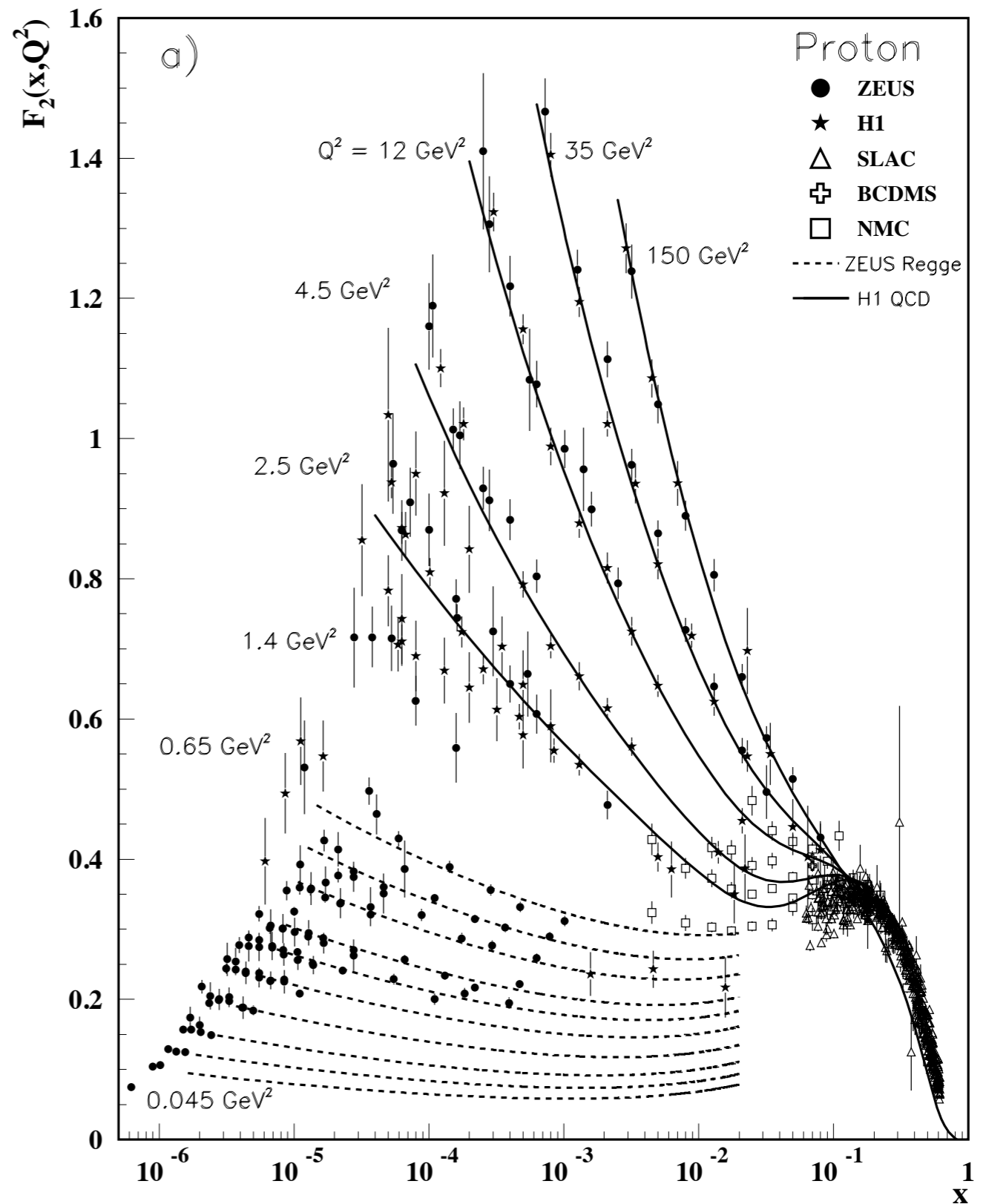
(source: PDG)



Measurements of $F_2(x, Q^2)$

- same data versus x

(source: PDG)



$e^+e^- \rightarrow \text{hadrons: jets}$

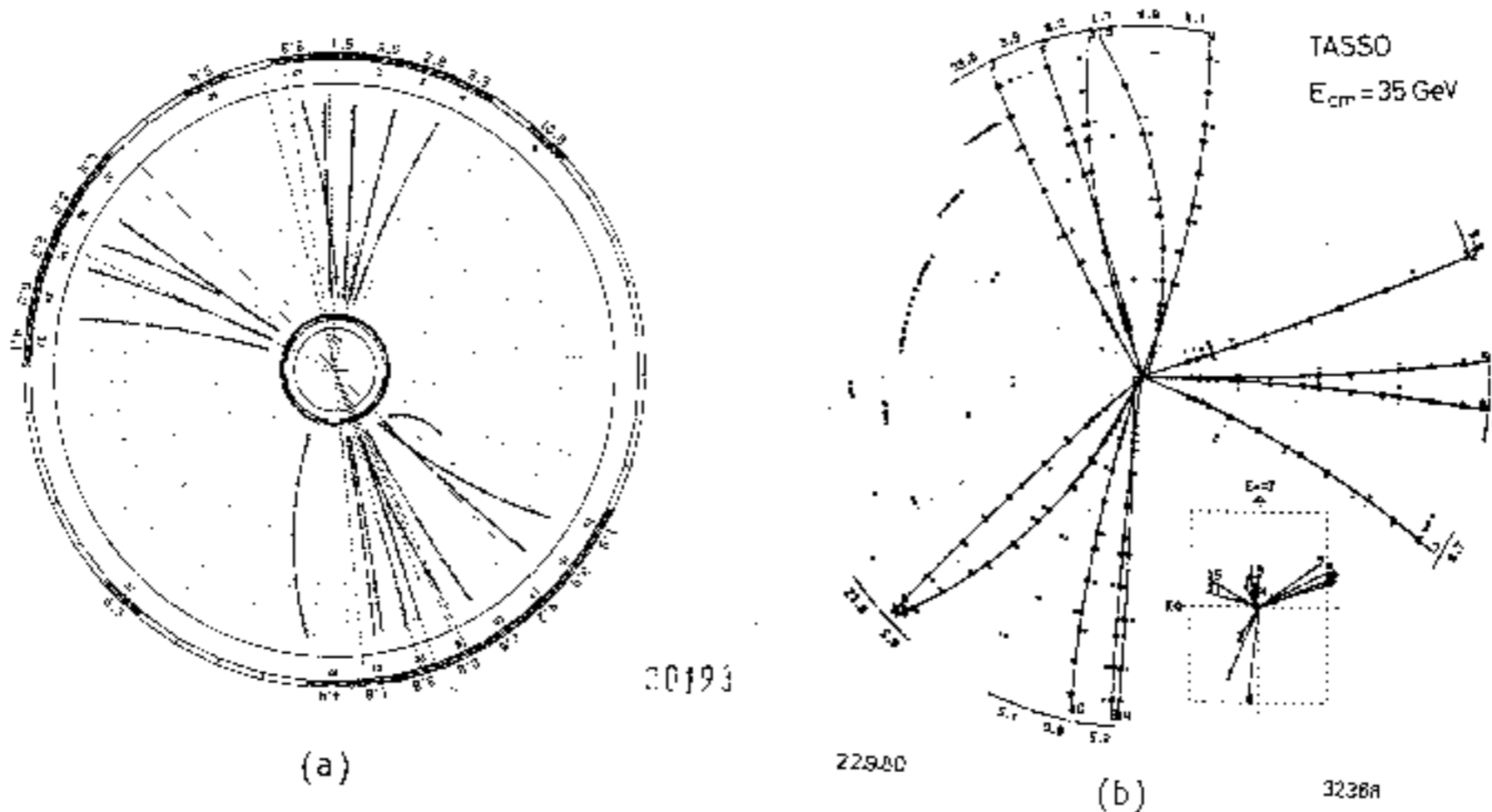


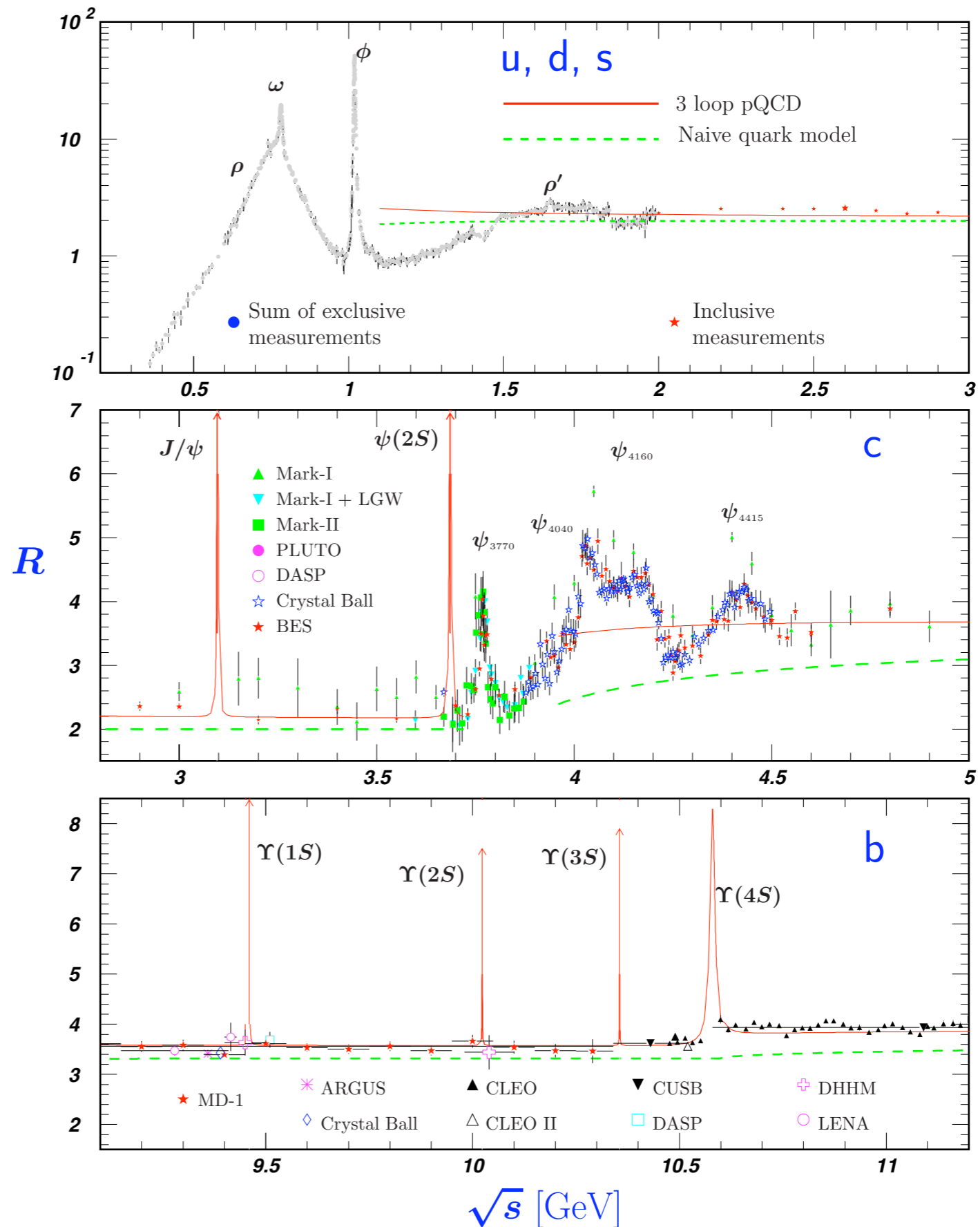
Fig. 3.24 Examples of three-jet events observed in the JADE and TASSO detectors as viewed along the beam axis. The insert in (b) shows a top view of the event.

Events with 3 jets: first direct evidence for the existence of the gluon

$e^+e^- \rightarrow \text{hadrons}$: cross section

normalised to
 $\sigma(e^+e^- \rightarrow \mu^+\mu^-)$

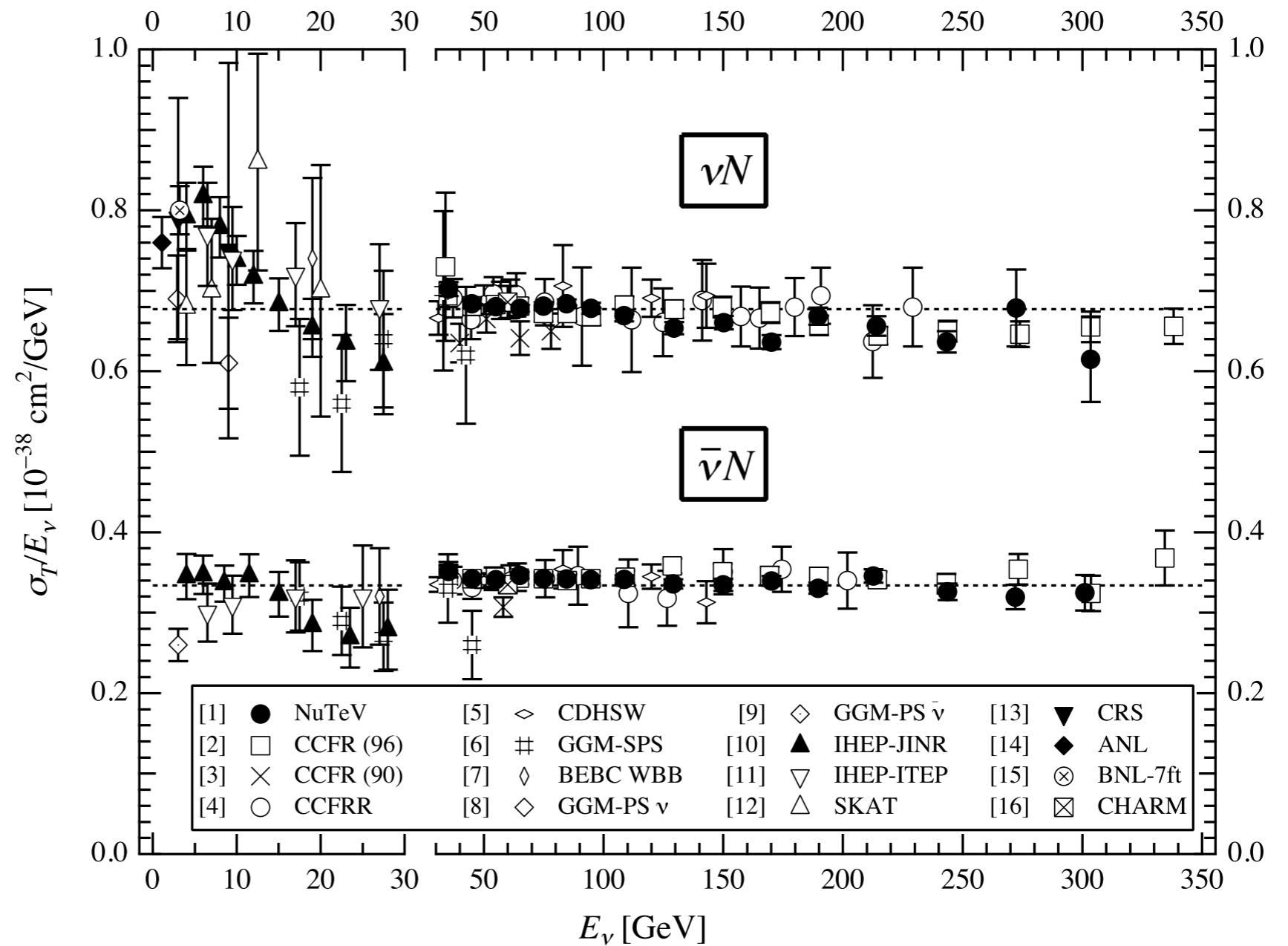
(source: PDG)



Week 7

Neutrino-nucleon scattering

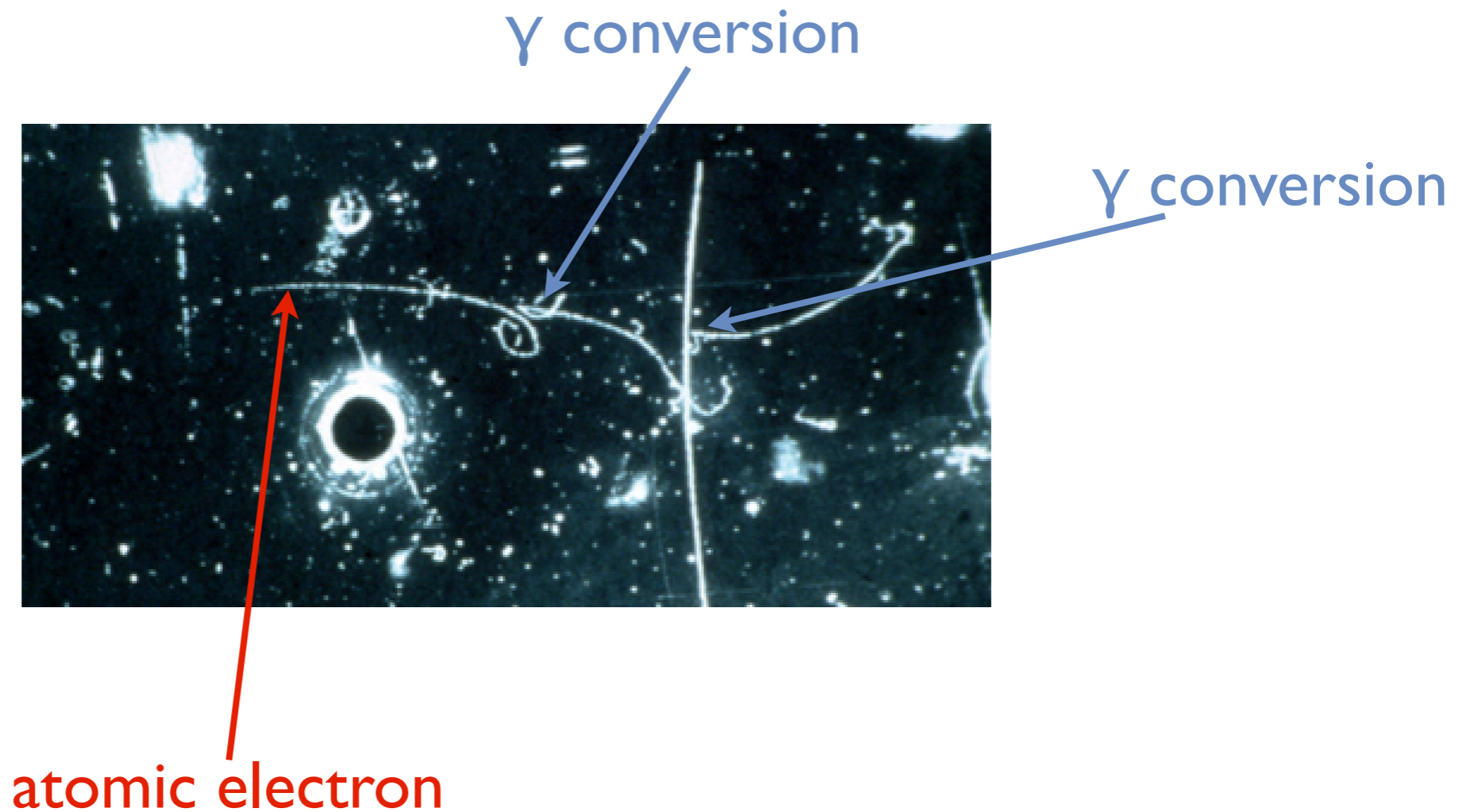
- in both cases: muon neutrinos
- shown: σ/E



(source: PDG)

Evidence for the Z boson

- Gargamelle experiment (bubble chamber), 1973

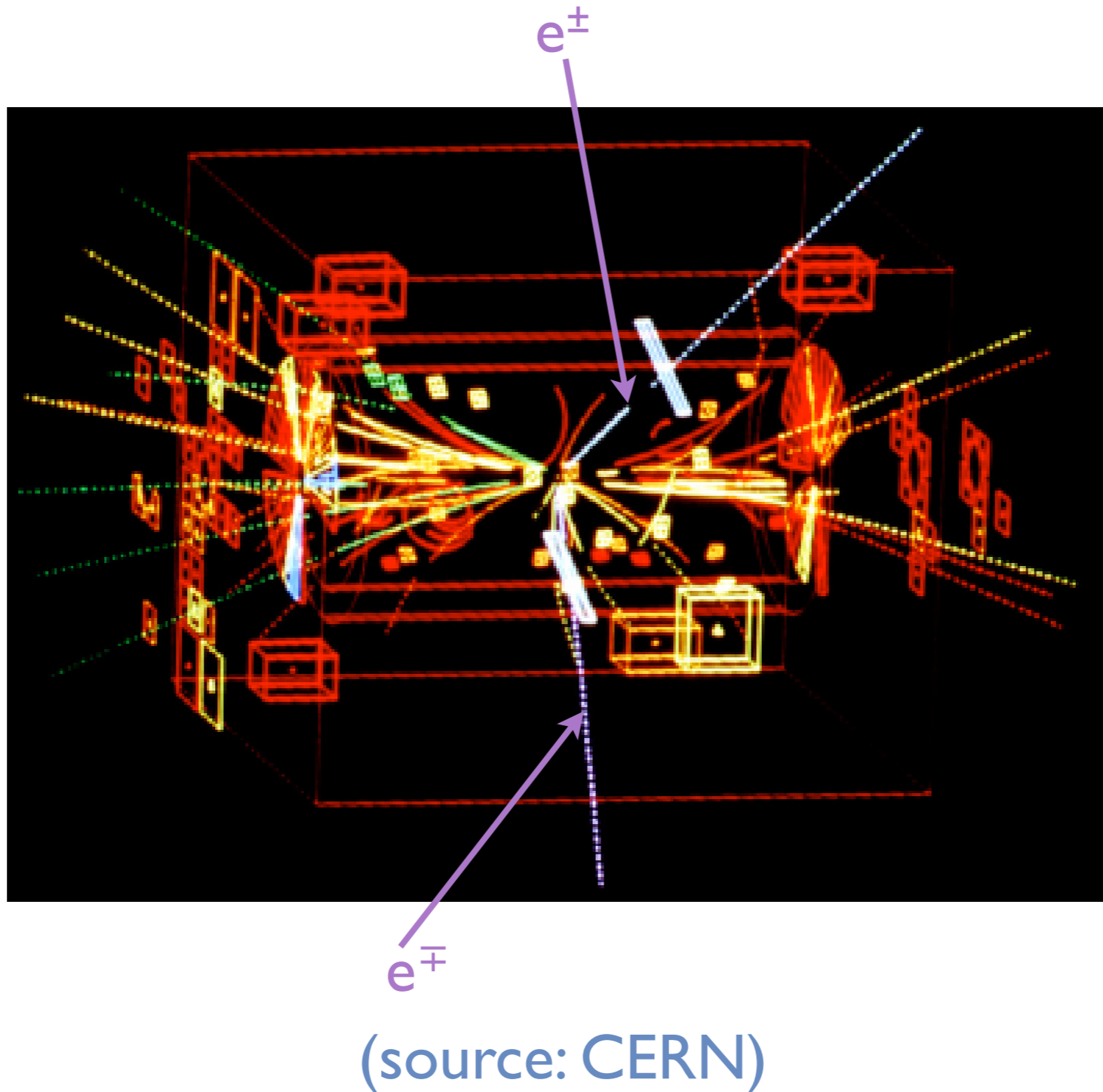


(source: CERN)

Week 8

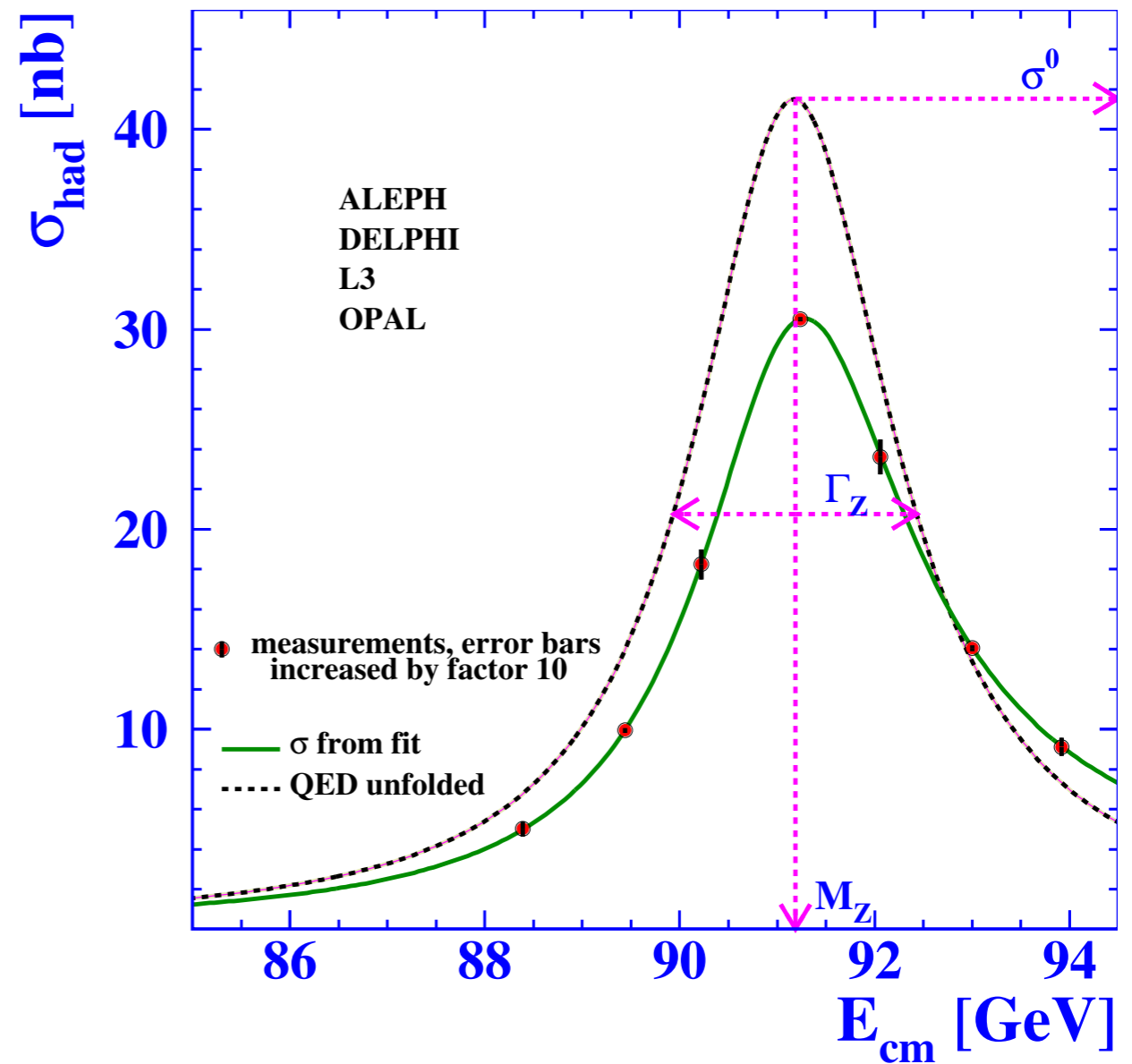
Discovery of the Z boson

- UAI experiment, 1983



Number of neutrino generations

- **Totale Z boson decay width**
 Γ_Z : width of the resonance
- **Partial decay width Γ_{had} :**
cross section at the peak of the resonance
- same for the decay to lepton pairs
- more complicated for decay to e^+e^- : **interference**
- Radiative corrections need to be applied!
- in particular, initial state photon radiation

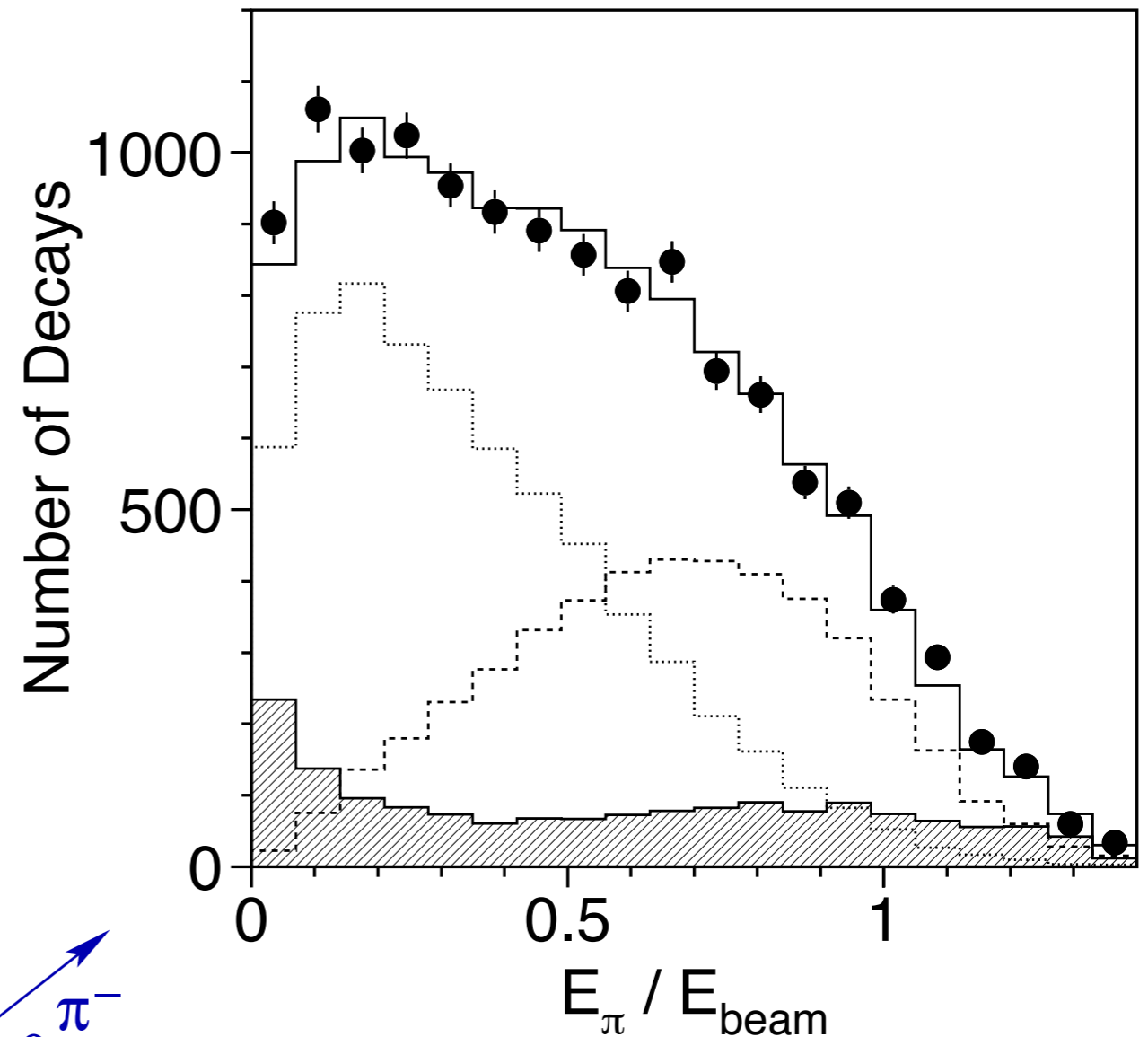
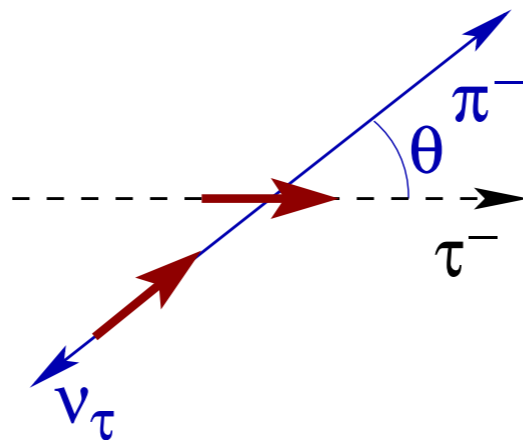


$$\Gamma_Z = \Gamma_{had} + \Gamma_{ll} + \Gamma_{\nu\bar{\nu}}$$

Extra slides

Parity violation as a tool

- $\tau^- \rightarrow \pi^- \nu_\tau$ decays
- E_π in the lab frame directly related to decay angle θ in the τ rest frame
- Used at LEP I to measure τ polarisation
- this too arises from parity violation, but in the production and decay of the Z boson



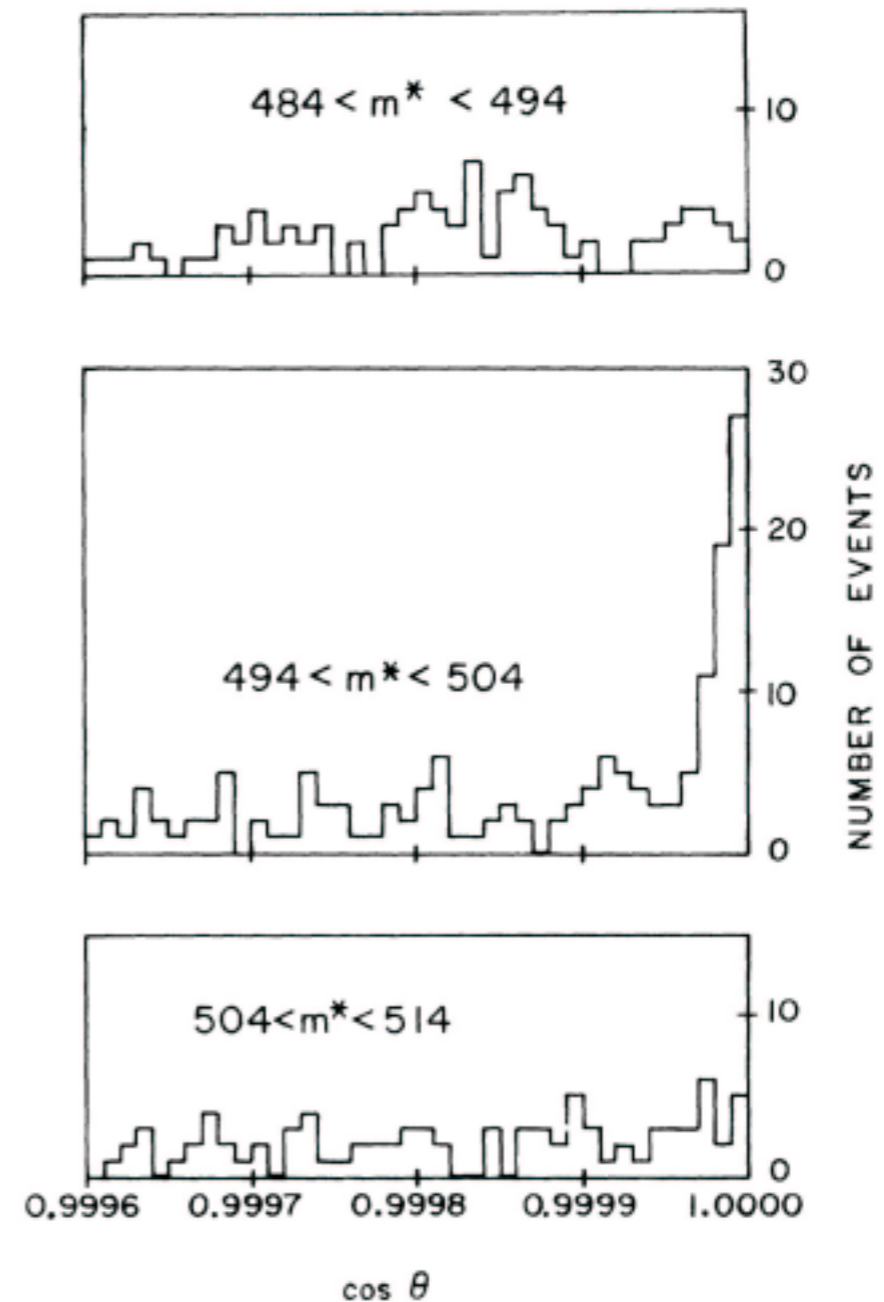
(source: CERN)

Evidence for the decay $K_L \rightarrow \pi^+ \pi^-$

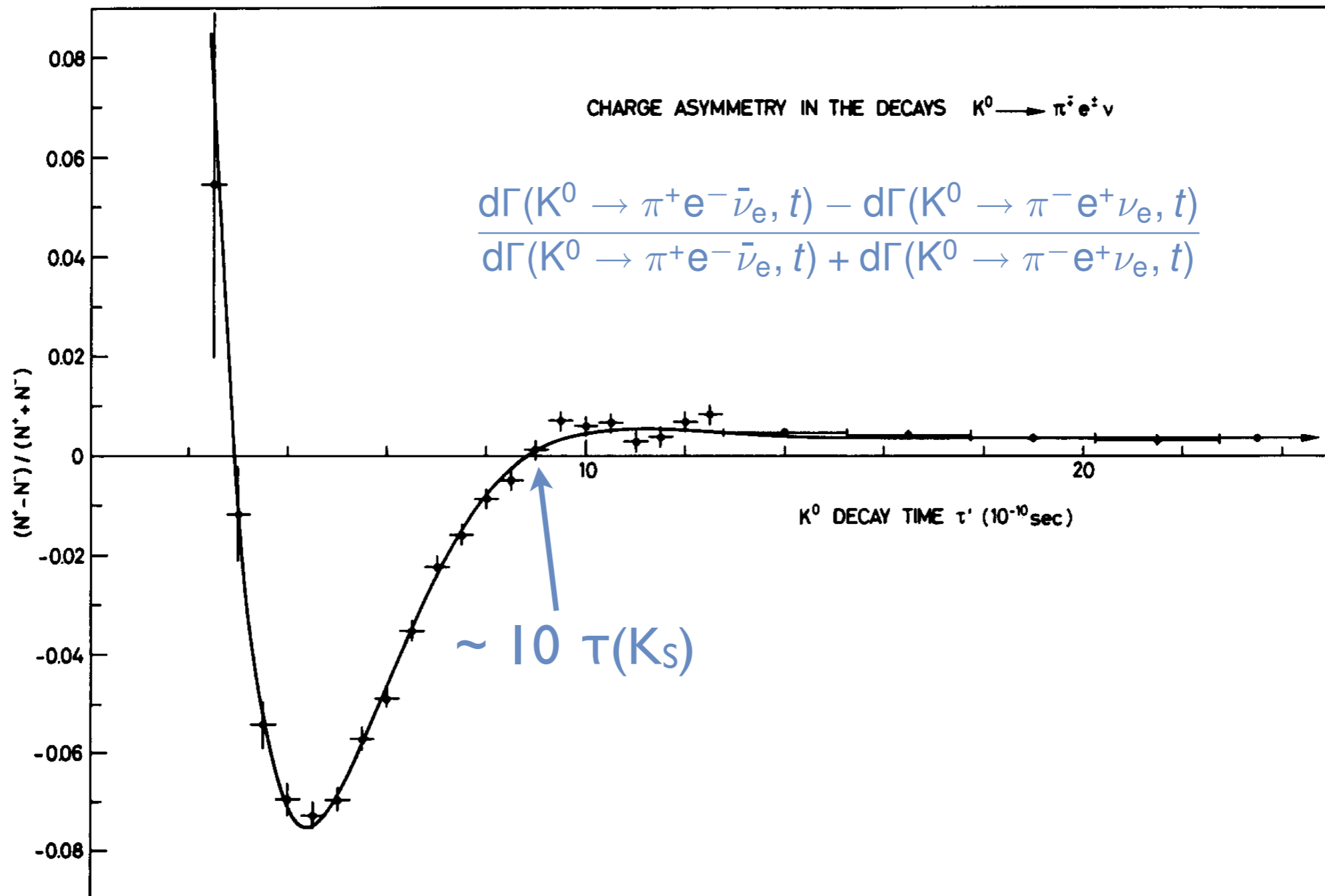
- Consider large decay times (so that only K_L remain)
- Reconstruct $\pi^+ \pi^-$ invariant mass (m^*) and direction with respect to the beam ($\cos\theta$)

**Kaons from the beam
clearly visible**

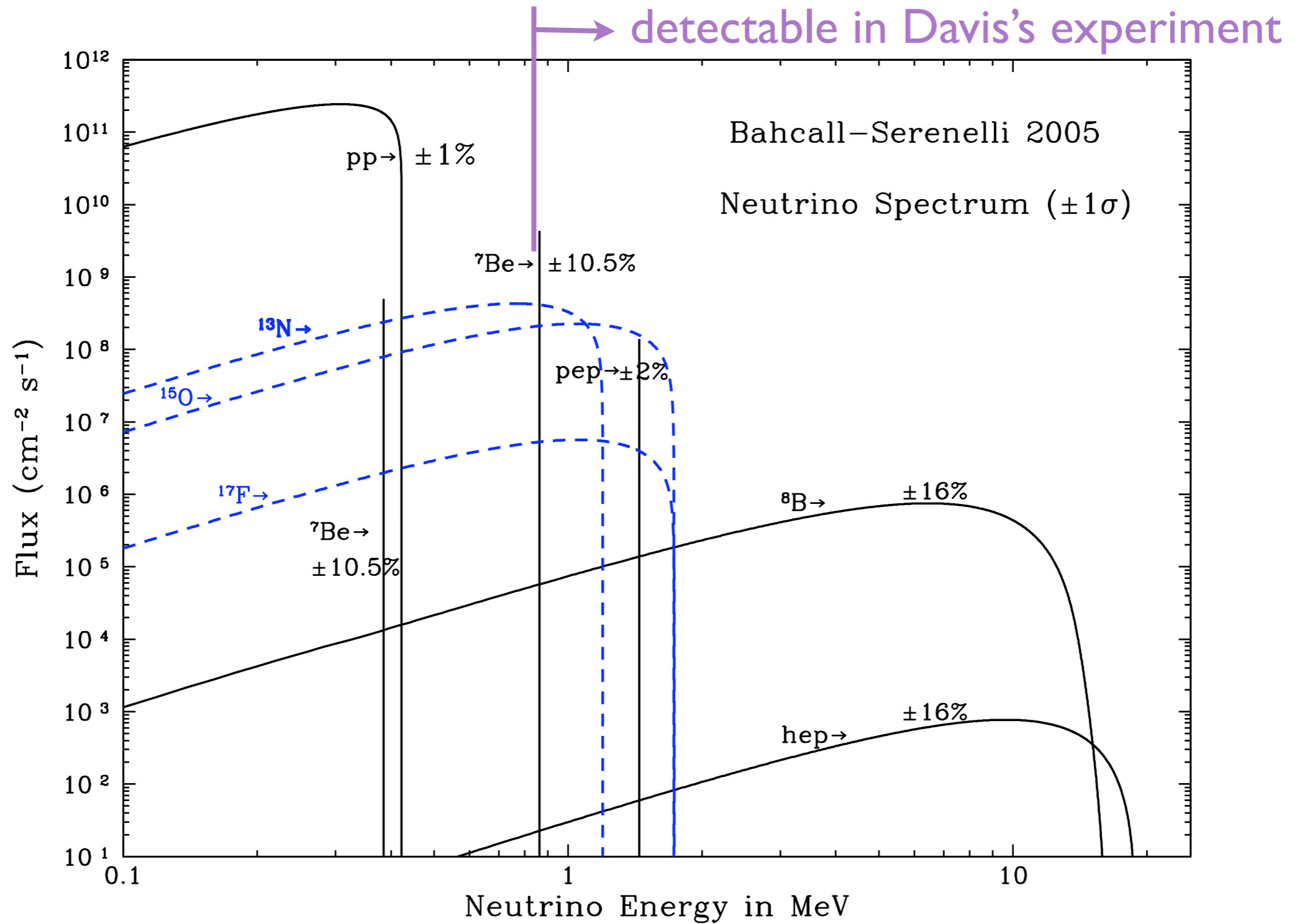
- other particles:
combinatorial backgrounds



CP violation in other decays

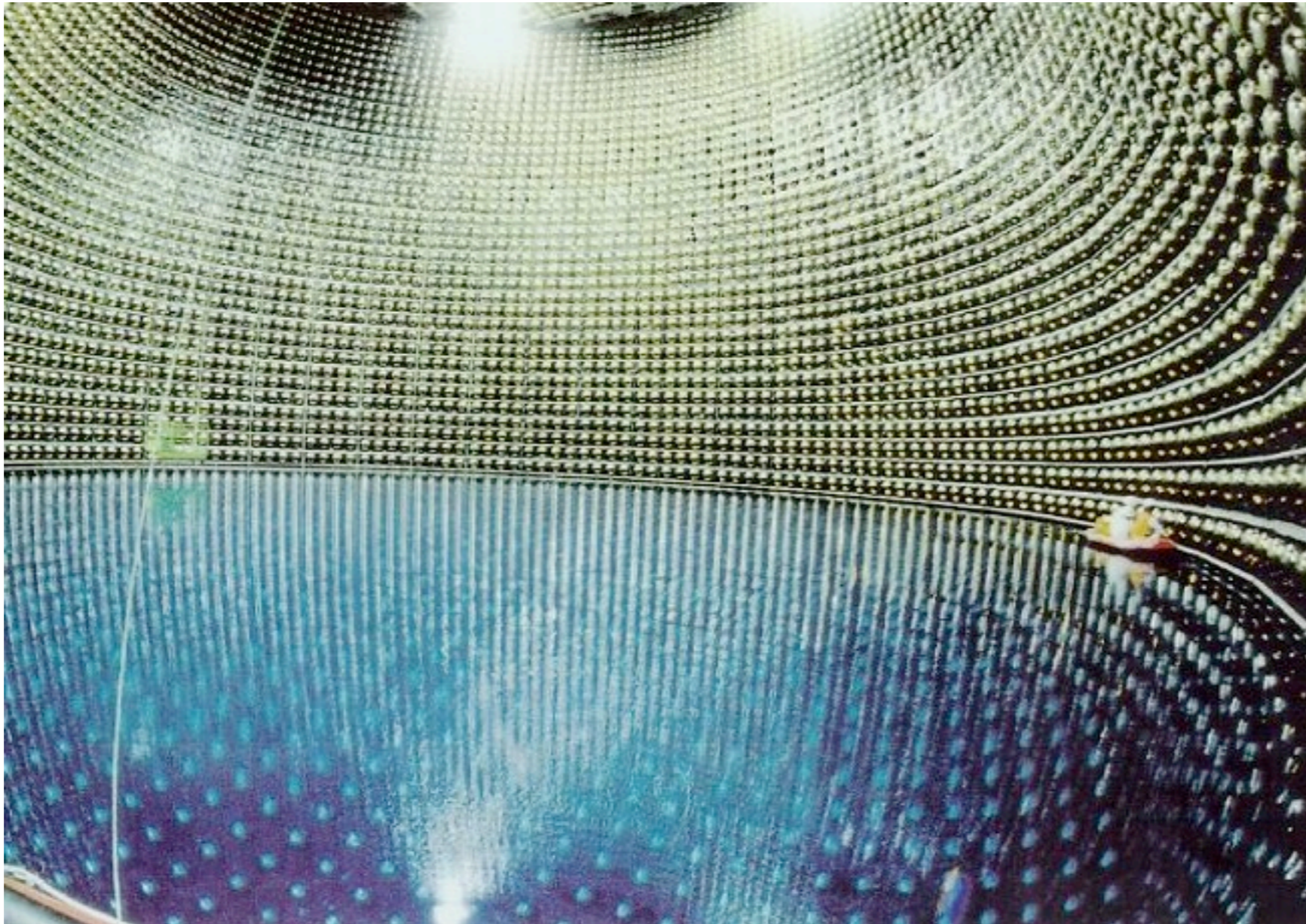


Solar neutrino flux

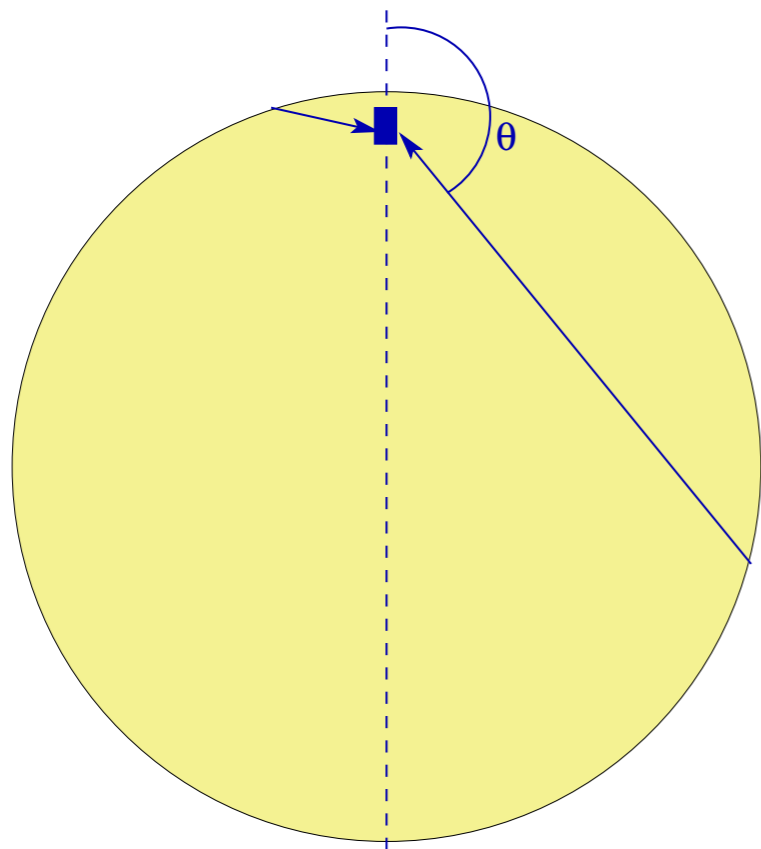


Super-Kamiokande detector

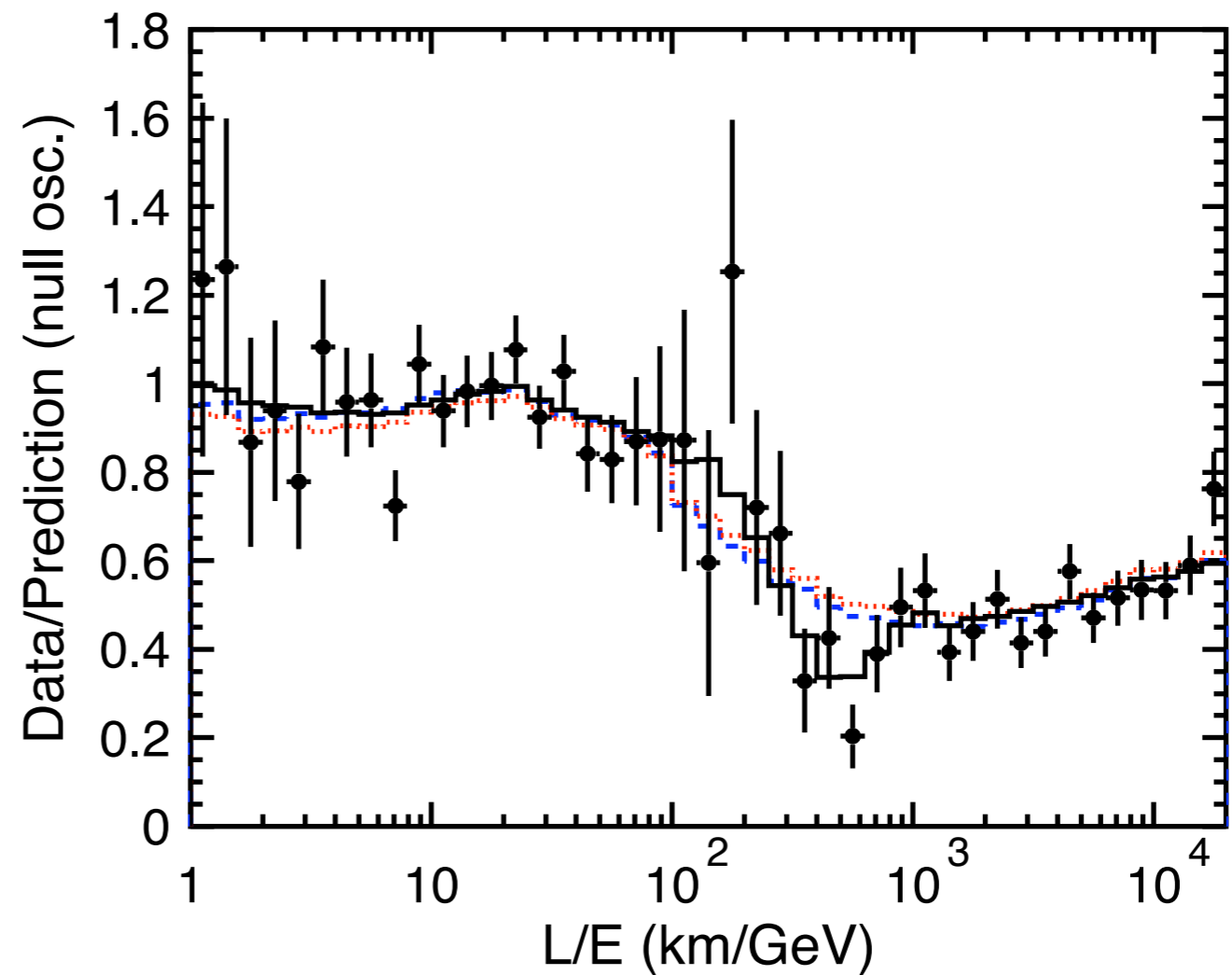
50 kton water, viewed by phototubes



Oscillations: Super-Kamiokande



relation between zenith angle and path length



Oscillations: KamLAND

